A SENSOR-LESS METHOD FOR DETECTING THE METHANOL CONCENTRATION IN AN OPEN-CATHODE DIRECT METHANOL FUEL CELL

By

AMIR REZA SHORAKA

A THESIS PRESENTED TO THE GRADUATE SCHOOL
OF THE UNIVERSITY OF FLORIDA IN PARTIAL FULFILLMENT
OF THE REQUIREMENTS FOR THE DEGREE OF
MASTER OF SCIENCE

UNIVERSITY OF FLORIDA

2012

To my family and friends for their love and support

ACKNOWLEDGMENTS

I would like to take this opportunity to express my thankful gratitude to my committee, Dr. William Lear, Dr. James Fletcher, and Dr. Oscar Crisalle for all their guidance, support, and encouragement. I owe my deepest gratitude to Dr. Joseph Campbell, Dr. Philip Cox, and my dear friend and colleague Jason Harrington. Without their help and advice this thesis would not have been possible. Also, I would like to thank all my friends and colleagues in the University of North Florida Fuel Cell Laboratory.

TABLE OF CONTENTS

page

LIST OF TABLES

LIST OF FIGURES

Abstract of Thesis Presented to the Graduate School
of the University of Florida in Partial Fulfillment of the
Requirements for the Degree of Master of Science

A SENSOR-LESS METHOD FOR DETECTING THE METHANOL CONCENTRATION IN AN OPEN-CATHODE DIRECT METHANOL FUEL CELL

By

Amir Reza Shoraka

August 2012

Chair: William E. Lear, Jr.
Major: Mechanical Engineering

Methanol concentration in the solution fuel plays an important role in maintaining the power output of a direct methanol fuel cell (DMFC) system. Hence, in most of the DMFC systems, in order to monitor and control the methanol concentration a concentration sensing method is used. In this research, a sensor-less methanol concentration sensing method for an open-cathode direct DMFC is discussed. In this method, the methanol concentration is detected by measuring the current density of the stack during the air-break period. Air-break is a common strategy to recover the temporary cathode performance loss during which the cathode air delivery is stopped and the stack operates at a constant voltage.

In comparison with a methanol concentration sensor an average difference of 0.068 M was reported over an operating temperature range of 45-55 ^{o}C and methanol concentration range of 0.3-1.5 M. Also, the effect of the stack life time, and the set voltage during the air-break was studied. One of the greatest features of this method is that it does not require any auxiliary device and since it is using the readily available

data during the air-break period it does not require any change in the normal load profile of the system.

CHAPTER 1
INTRODUCTION

Increasing demand for power sources in portable applications such as cell phones and laptops has revealed the necessity for developing technologies other than the conventional batteries. Currently, primary (disposable) and secondary (rechargeable) batteries are widely used and well established as the power source for portable applications. However, the demand for portable power has been increasing faster than the battery technologies and capabilities. This has attracted a global attention to fuel cells, which potentially offer a higher power density, and longer lifespan [1].

Among the different types of the fuel cells, direct methanol fuel cells (DMFCs) are considered to be the most promising fuel cell system for the commercialization purposes in the short term, particularly for small to mid-size portable applications such as laptops. One of the main reasons for this is attributed to the fuel used in DMFCs, liquid methanol. Methanol is a high energy-density fuel (15700 kJ/l), easy to handle, transport, and store, and can be produced from various sources such as fossil fuels and biomass. In addition, low operating temperature (typically between 30 ^{o}C to 120 ^{o}C), lack of separate fuel reformer, ease of re-fueling and compactness are among other features of DMFCs [2]. Even in comparison with the Li-Ion batteries, in terms of the gravimetric and volumetric efficiency, DMFCs show better performance in long term operations [2].

However, DMFCs suffer from several drawbacks including the following: the expensive platinum-based catalyst required for both the anode and cathode sides, and methanol crossover from anode to cathode, which wastes the fuel and lower the system fuel efficiency [2].

Background

DMFC Performance

In a DMFC, the electrochemical reaction between methanol and water in the anode produces hydrogen ions, electrons, and carbon dioxide (CO_2). The electrons flow through an external circuit while the hydrogen ions diffuse through the electrolyte membrane to the cathode side, Equation 1-1. At the cathode, the electrons and the hydrogen ions complete the reduction reaction at the presence of oxygen from air, Equation 1-2. The overall reaction is shown in Equation 1-3.

$$CH_3OH + H_2O \rightarrow 6H^+ + 6e^- + CO_2 \quad \text{(Anode)} \quad (1\text{-}1)$$

$$6e^- + 6H^+ + 1.5O_2 \rightarrow 3H_2O \quad \text{(Cathode)} \quad (1\text{-}2)$$

$$CH_3OH + 1.5O_2 \rightarrow 2H_2O + CO_2 \quad \text{(Overall cell)} \quad (1\text{-}3)$$

A single cell DMFC in operation is depicted in Figure 1-1 DMFC single cells can be combined in series (or parallel) configurations to form stacks to achieve a desired power output.

Polarization Curve and Performance Losses

The performance of a fuel cell is typically depicted with a graph of its current-voltage characteristics, called the polarization curve [3]. The polarization curve shows the output voltage for any given current density imposed on the fuel cell. A typical polarization curve is shown in Figure 1-2. The theoretical thermodynamic open circuit voltage (OCV) for a fuel cell can be calculated by the following equation:

$$E = \frac{-\Delta g_f}{nF} \quad (1\text{-}4)$$

where *E* is the theoretical thermodynamic OCV, Δg_f is the change in the free energy for the reaction, *n* is the number of transferred electrons per molecule of fuel reacted (6 in case of DMFC), and *F* is the Faraday constant (96486 coulomb/mol e^-).

An ideal fuel cell would sustain the theoretical OCV at any current density (as long as fuel is supplied). However, due to kinetic issues which cause losses, the actual voltage output of a real fuel cell is lower than the theoretical thermodynamic value. Three regions can be distinguished in Figure 1-2 and in each region a certain type of loss is dominant. Activation losses are caused by the slowness of the electrochemical reactions on the surface of the electrodes and a portion of the theoretical OCV is lost to drive these reactions. Ohmic losses are the drop in the voltage due to resistance to the flow of electrons and ions through the electrode materials and the membrane. Mass transport or concentration losses are the result of the reduction of the fuel concentration or a failure to transport sufficient fuel to the electrodes [4].

Membrane Electrode Assembly (MEA)

The overall performance of a DMFC is highly dependent on the membrane electrode assembly (MEA) and its structure [5]. The MEA structure (Figure 1-3) is constructed from several layers:

Gas diffusion layer (GDL) is a layer that provides paths for the reactants (methanol, water, and oxygen) to reach to the electrode surfaces and also for the products (CO_2 and water vapor) to leave the electrode surfaces. The GDL must be conductive and porous and the most common material used for the GDL is carbon [6].

The electrolyte membrane used in DMFC's is polymer electrolyte membrane (PEM). The PEM provides an ionic conductive medium for the protons, separates the

reactants, and acts as an electrical insulator for conduction of electrons. A desirable electrolyte membrane must have high proton conductivity, low methanol crossover (MCO), and must be chemically and electrochemically stable under operating conditions [7]. Nafion, a poly(tetrafluoroethylene) based ionomer [8], is known as the standard electrolyte for DMFC because of its great proton conductivity, electrochemical stability, and durability; however it suffers from high methanol permeability and water drag which can cause cathode flooding [7]. Neburchilov [9] discussed the recent progress in the new membranes for DMFC's and concluded that the hydrocarbon membranes seem to have advantages in comparison with Nafion with reduced MCO, increased methanol utilization, smaller water drag number (number of the water molecules dragged with each proton), and possibly improved dimensional stability [7].

The anode catalyst layer is where the methanol electro-oxidation reaction (MOR) occurs. The catalytic electro-oxidation reaction between methanol and water that results in electron and proton liberation and CO_2 formation occurs at the presence of platinum (Pt) catalyst. The methanol electro-oxidation reaction is a complex sequence of reactions [10] and carbon monoxide (CO) is the most stable intermediate formed. CO is considered a catalyst since it is quickly absorbed to the catalyst, and drastically reduces the active catalysts sites. In order to overcome this problem, a second catalyst must be used. A combination of platinum and ruthenium (Ru) is the most active combination for DMFC [5,11].

The cathode catalyst layer is where the oxygen reduction reaction (ORR) occurs. The most common catalyst for the cathode is platinum (Pt). Protons, liberated in the

anodic reaction, transfer through the membrane and reach the cathode to complete the ORR with the electrons and oxygen, Equation 1-2.

DMFC systems

In addition to the DMFC stack, a complete DMFC system requires several peripheral components such as pumps, fan/blower, filter, etc. These periphery components are referred as the balance of plant (BOP). Depending on the cathode design, two types of DMFC systems can be identified: closed-cathode or conventional (Figure 1-4) and open- cathode (Figure 1-5) [12].

Water management is a critical issue in a DMFC system particularly for portable applications. In order to keep the balance between the water consumption in the anode, and the water formation in the cathode, a portion of the water formed in the cathode reaction must be recovered. In a conventional closed-cathode DMFC system, in order to recover the water in the cathode exhaust air, auxiliary water recovery components are required. However, these components are large and cumbersome and also do not directly aid the electrochemical process. In an open-cathode DMFC system, by addition of a hydrophobic liquid barrier layer between the cathode catalyst layer and the cathode gas diffusion layer in the MEA structure, the water recovery is taken place within the MEA. This is a great advantage of an open-cathode configuration which eliminates the bulky water recovery components required for the conventional configuration.

Motivations and Objectives

Motivations

The methanol concentration in the anodic fuel solution plays an important role in the performance and power output of DMFCs [13,14]. In order to maintain the optimum power output of a DMFC, maintaining the methanol concentration in the fuel solution

within a predetermined range is required. If the methanol concentration falls lower than the optimum range, it can cause fuel starvation in the anode which causes damage to the anodic catalyst layer. However, if the methanol concentration exceeds the optimum range, it increases the methanol crossover to the cathode side, where it can directly react with oxygen within the cathode catalyst layer. Since methanol crossover is a waste of fuel, it adversely affects the fuel system efficiency. Also, methanol crossover decreases the cathode potential because of the mixed potential. In the DMFC, cathode potential deteriorates as a result of the depolarization effect caused by methanol crossover [15]. Hence, in order to maintain the power output of a DMFC system within an optimum range, monitoring and controlling methanol concentration in the fuel is required.

In general, the existing methanol concentration sensors are hard to miniaturize, might require auxiliary driving devices which add complexity to the system, and costly. These would significantly limit their application particularly for portable DMFC systems. For instance, the methanol concentration sensor used in UNF DMFC [12] system accounts for roughly 10% of the system total volume and one third of the system cost.

However, since the DMFC performance is dependent on methanol concentration, there is an opportunity to determine the methanol concentration by analyzing the DMFC operating characteristics such as voltage or current. However, the DMFC performance is also dependent on other variables such as the operating temperature and operating time. This could complicate establishing a relationship between methanol concentration and DMFC performance characteristics particularly during normal operation. Another opportunity to determine methanol concentration is during the rejuvenation or air-break

period [16,17]. Air-break is a strategy to partially recover the performance loss in DMFCs and is performed by stopping the cathode air delivery while the voltage is set to a fixed value.

Objectives

The purpose of this thesis is to explore the dependence, in an open cathode DMFC, of the current density during the rejuvenation period at a constant voltage on the methanol concentration. Based on this, the feasibility of a sensor-less method to detect the methanol concentration is to be explored, in which the methanol concentration in the fuel is determined by measuring the current density during the rejuvenation period. In addition, the effect of the rejuvenation voltage set-point, the operating temperature, and the stack life time on this method is to be determined.

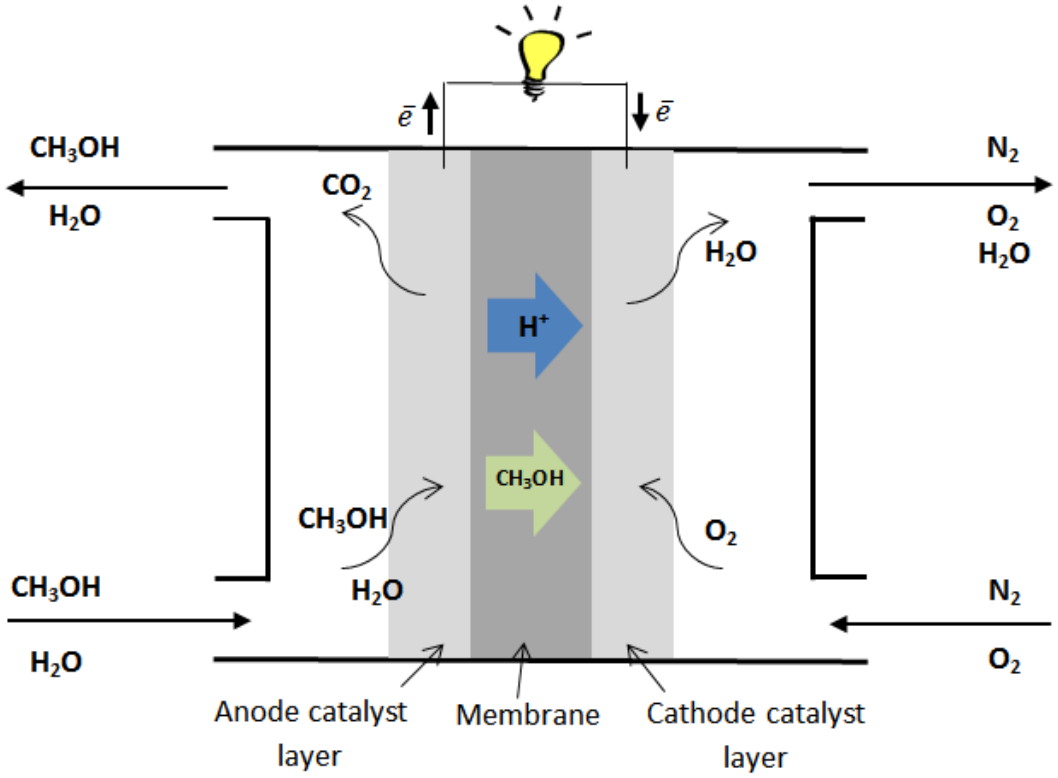

Figure 1-1. Basic scheme of the DMFC.

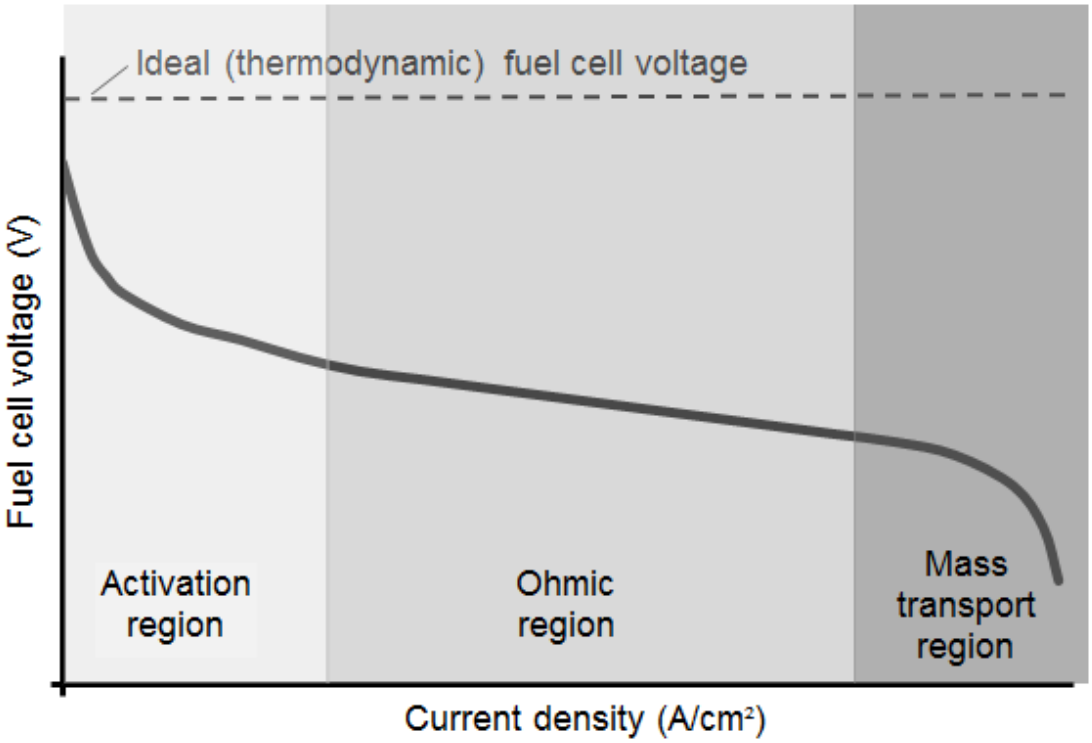

Figure 1-2. Polarization curve.

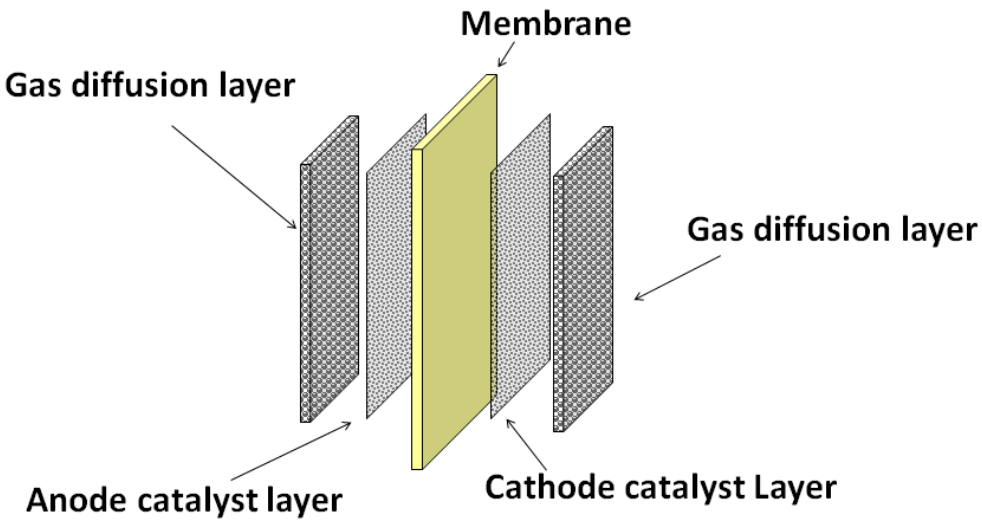

Figure 1-3. Membrane electrode assembly (MEA).

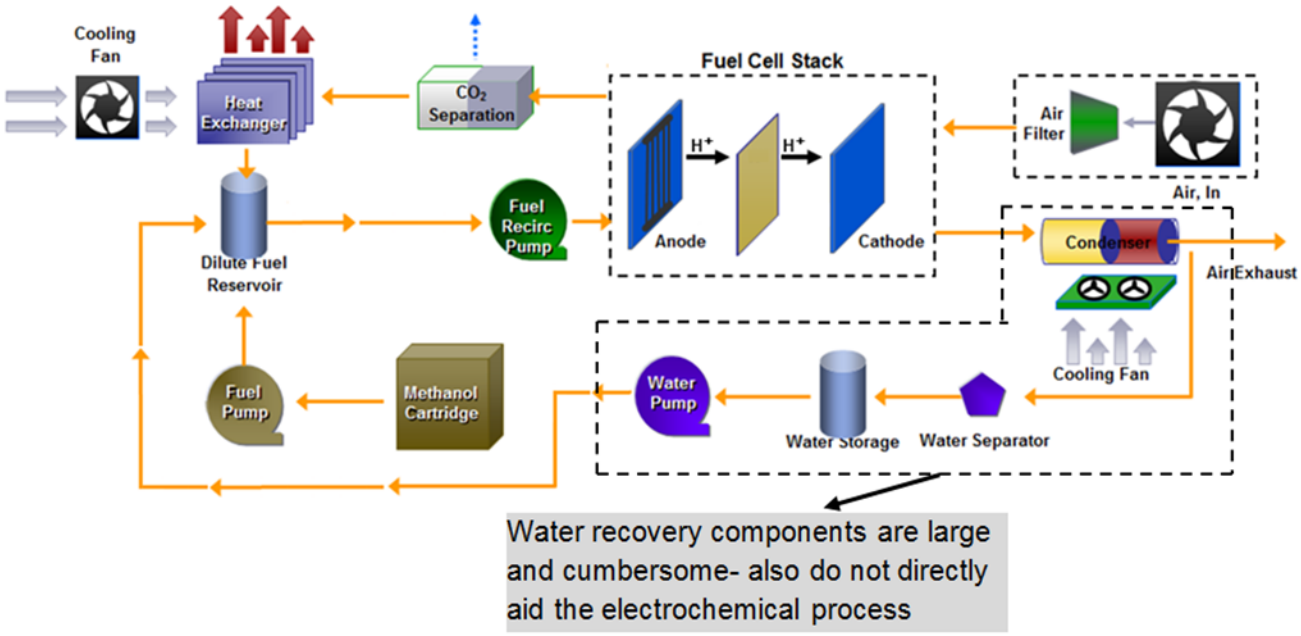

Figure 1-4. A conventional (closed-cathode) DMFC system. Reprinted by permission from Dr. James Fletcher, 2012, Advanced direct methanol fuel cell for mobile computing, University of North Florida.

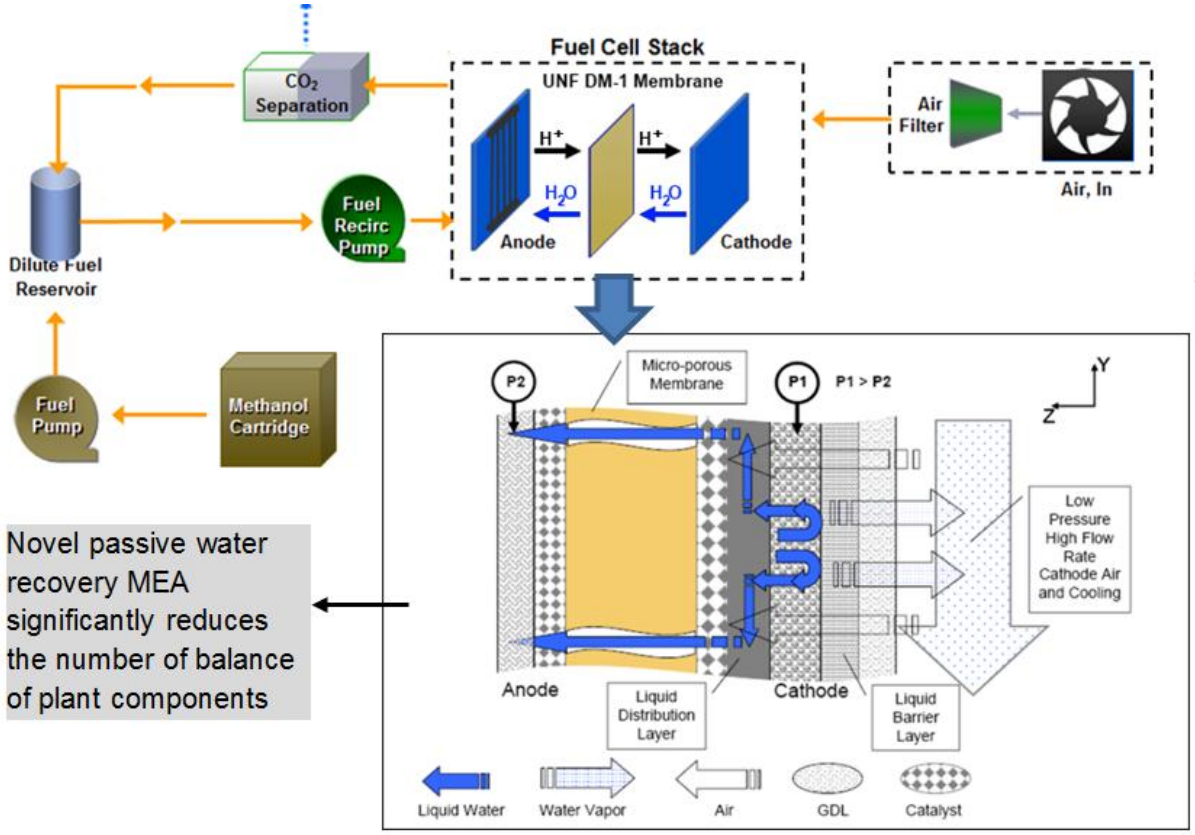

Figure 1-5. An open-cathode DMFC system. Reprinted by permission from Dr. James Fletcher, 2012, Advanced direct methanol fuel cell for mobile computing, University of North Florida.

CHAPTER 2
LITERATURE REVIEW

In this chapter the literature review for different types of methanol concentration sensing methods is presented. The methanol concentration techniques can be categorized into three groups: electrochemical sensing methods, physical sensing methods, and sensor-less sensing methods.

The requirements for a suitable methanol concentration sensor can be summarized as [13]:

- wide methanol sensing range of up to 5 M,
- high resolution and accuracy around the operating point,
- in-line operation and rapid response,
- tolerance to metallic ion impurities such as Fe^{3+} and Cu^{2+},
- ideally tolerance to the dissolved CO_2 and CO_2 bubbles,
- long-term stability,
- wide range of operating temperature,
- amenable to miniaturization for tight packaging and system integration.

Electrochemical Sensing Methods

In principle, an electrochemical sensor is a small DMFC that its performance is used as the sensing measurement. Depending on the reaction mechanism, there are two types of electrochemical sensors: oxidation current (electrolytic type) and fuel cell-based (galvanic type) [13].

The relationship between methanol concentration and methanol oxidation current is described in [18,19] by Narayanan. In this sensor the methanol oxidation current under a constant anodic potential is used as the sensing signal. The oxidation current is dependent on methanol concentration in the fuel solution. The sensor is suitable for methanol concentration range of 0.25-2.0 M with an average error of 0.02 M during an

entire 70 hour test for a circulating solution stream of 0.5 M. The temperature dependency of this method is not clearly discussed.

An alternating pulse electrochemical methanol concentration sensor is described in [20]. The operation of this sensor is based on measuring the methanol oxidation current. In this sensor, the structure of both electrodes is the same and methanol solution is fed into both electrodes simultaneously. Alternative pulse signal changes the potentials at the working electrode and counter electrode of the sensor in a certain frequency. Hence, methanol oxidation and hydrogen evolution occur on the same electrode alternately. This method has effective measurement in the range of 0-2.0 M. It is reported that the required power for this sensor is 1.5 W and the time response is 20 seconds.

A miniaturized electrochemical methanol sensor is discussed in [21]. The sensing principle is based on measuring the methanol oxidation current. In this sensor, reduction of size is made possible by eliminating both the gas diffusion backings and any housing part needed for physical integrity of the unit. It is reported that this sensor is suitable for methanol concentration range of 0.5-3.0 M and the temperature range of room temperature to 80 $^{\circ}$C. The total power consumption by the sensor is 1 mW and the sensor responds within few seconds to the concentration changes.

A fuel cell-base (galvanic type) methanol concentration sensor is discussed in [22]. This sensor is essentially a passive DMFC. The MEA for this sensor is uniquely designed to have the anode side much smaller than that of the cathode. This is to ensure that all the methanol diffuses to the anode/membrane interface can be completely reacted, thus the measured sensor current reflects the true concentration of

the solution. It is claimed that this sensor is able to operate over a 20-80 ^{o}C temperature range and a methanol concentration range of 0-4 M. This sensor has a linear relationship in calibration under a constant temperature and also a first order correlation with respect to the temperature change.

A fuel cell-based methanol concentration sensor is explained in US patent 4,810,597 [23]. The operation principle of this particular sensor is based on measuring the open circuit voltage of the cell. The methanol crossover is directly related to the solution fuel concentration in the anode side. So, the mixed potential, which reduces the cathode potential and is caused by the methanol crossover, is larger for the case of higher concentration in the anode side. This means the methanol concentration at the anode can be determined by measuring the open circuit voltage of the cell. However, the change in the open circuit voltage is not significant over a range of methanol concentration of 0.25-5.0 M.

Instead of measuring the open circuit voltage of the sensing cell, in US patent 5,624,538 [24], the cell voltage at a constant load of 1 ohm is used as the sensing measurement to determine the methanol concentration. The method is suitable for concentrations only up to 1 M. To extend the measuring range of this method, a new method was introduced in US patent 6,527,943 [25] in which the methanol concentration range was extended to 4 M. This sensor is claimed to have an operating temperature range of 40-100 ^{o}C.

The fuel cell-based methanol concentration sensor described in [26] is a small passive DMFC. In this method the methanol concentration is determined by measuring the cell temperature. It is shown in [26] that there is a linear relationship between the

maximum temperature rise of the sensor and methanol concentration in the range of 0.5-10.0 M.

The feasibility of using single-walled carbon nanotube (SWCNT)/Nafion composites as methanol sensors is discussed in [27]. In this method, methanol concentration is determined by measuring the resistance of the sensor under a constant voltage. The result for a range of methanol concentration of 0.5-5.0 M is presented in [27].

Physical Sensing Methods

The physical properties of aqueous methanol solution have been investigated and measured using several different approaches [13]. The physical properties of aqueous methanol solution, such as density, viscosity, relative dielectric constant, heat capacity, and speed of sound are dependent on the methanol concentration in the solution.

A density type sensor is discussed in [28]. In this sensor the resonant frequency of a solution sample is used to determine the sample density. The resonant frequency of vibration of the sample changes as the result of the change in the mass of the samples. This sensor operates over the entire range of concentrations. This sensor is not specifically designed for DMFC systems.

A micro-electro-mechanical system (MEMS)-based methanol concentration sensor designed for DMFC systems is discussed in [29]. This sensor is based on a vacuum packaged resonant microtube and an on-chip platinum temperature sensor to measure the density of the solution sample. For a methanol concentration range of 0.6-3.0 M and a temperature range of 10-50 ^{o}C, this sensor is found to have a linear relationship. Also, formic acid contaminants under concentration of 100 ppm do not

affect the accuracy of this sensor [29]. This sensor is used in a DMFC system developed by the University of North Florida (UNF) [12].

The dielectric property of the aqueous methanol solution was investigated in [30] and it is shown that the static dielectric constant changes with variation in the methanol concentration. By measuring the frequency-dependent capacitance, the dielectric constant can be determined. This type of sensor consists of a capacitor that comprises a pair of spaced electrode plates. By measuring the capacitance as the fuel passes through the electrodes, the dielectric constant is determined. The dielectric spectra for a methanol concentration range of 0-5 %wt (about 0-1.6 M) were measured by Doerner [31].

A viscosity type sensor was introduced in US Patent 6,536,262 [32] .The viscosity of aqueous methanol solution is dependent on the methanol concentration of the solution and in the range of 0.0-9.0 M a linear relationship can be seen. In this sensor, the viscosity of the sample is determined by measuring the pressure across the constriction with a constant laminar flow rate. Due to the shape of the viscosity-concentration curve, double value could be a problem. But this may not be an issue for the DMFCs since the recommended methanol concentration in the fuel is less than 1.5-2.0 M for DMFCs [33].

The speed of sound in the methanol solution is related to its density and elastic properties [34]. In the US Patent 6,748,793 [35], an ultrasound method for determining the methanol concentration in an aqueous solution is discussed that can determine the methanol concentration in the range of 0.1-5.0 wt% (about 0-1.6 M). In this sensor a piezoelectric transducer was used to emit and receive ultrasound waves. Using similar

reference and sample chambers, the differential propagation time of the ultrasound pulses was measured in response to the change of methanol concentration. Evaluation of ultrasonic sensing of methanol concentration for DMFC over a methanol concentration range of 0-15 wt% (about 0-5.0 M) and a temperature range of 25-78 ^{o}C is discussed in [36]. The results show that the propagation distance and equipment sampling rate affect the accuracy of sound speed measuring.

An infrared spectrum type sensor is discussed in US Patent 6,815,682 [37]. The transmittance of infrared radiation is a function of the methanol concentration in the solution. This sensor is reported to have effective measurement over a range of methanol concentration of 0.0-5.0 wt% (about 0-1.6 M) with an accuracy of 0.1 wt% (about 0.03 M). This sensor has high accuracy particularly for methanol concentration less than 1.0 M.

There are several methanol concentration sensing methods that work based on measuring the refractive index [38, 39]. The NeHe laser-based technique proposed in [38] can determine the methanol concentration in the solution over the entire range of concentration with a precision on the order of 0.01 wt% [13].

The specific heat capacity of an aqueous methanol solution is dependent on methanol concentration of the solution. Hence, the technique introduced in [40] determines the methanol concentration by measuring the specific heat capacity of the solution. A temperature difference of approximately 2 ^{o}C was reported for a change of methanol concentration from 0.5 M to 1,0 M with a flow rate of 100 mL/min to the sensor [13].

A methanol sensor using a shear horizontal surface acoustic wave device is explained in [41]. A linear relationship between the sensor response and concentration was obtained over a temperature range of 25-60 ^{o}C and concentration range of 0-50 wt% (about 0-16 M). The reported accuracy was 0.1 %wt.

The nonlinear frequency response of a DMFC is studied by analyzing the total harmonic distortion (THD) spectra in [42]. The results show that there is a monotonic correlation between THD values and methanol concentration at certain frequencies. The sensitivity of this correlation is improved with increased current amplitude. This correlation for methanol concentration range of 0.3-1.0 M is presented in [42].

Sensor-less Methods

Other than the conventional methods of employing a methanol concentration sensor as discussed in the previous sections, there are several works that focus on sensor-less methods in order to control the operation of the fuel cell. In a sensor-less method, the methanol concentration is determined based on a known relationship between the fuel cell performance characteristics and the methanol concentration [13].

A strategy of estimating methanol concentration in a DMFC system is explained in [43]. The algorithm of estimating methanol concentration is developed by using a three-dimensional measurement space and constant concentration surface (CCS). The three indices are chosen to be current, voltage, and temperature. This method can estimate the methanol concentration without interrupting the operation of the system. The reported error over a concentration range of 3.5-5.5 vol.% (about 0.85-1.40 M) and temperature range of 30-55 ^{o}C is 0.3 vol.% (about 0.075 M).

A modified and more advanced form of the method discussed in [43] is explained in [44] where a compensation scheme is proposed and validated to overcome the

voltage decay limitation in the method described in [43]. Also, an approach to evaluate the consumption rate of water and methanol is provided in [44].

A sensor-less method of controlling the methanol concentration in DMFC, which is based on estimating the methanol consumption rate in the system, is explained in [45]. The total rate of methanol consumption is calculated based on the fuel cell current and the estimated rate of methanol crossover. The average error at operating temperature of 60 ^{o}C was within 20% of the set points (0.4 M and 0.8 M).

In the proposed method in [46], the methanol concentration is regulated by using feedback from voltage measurements. This paper concluded that at a constant current density, steadily increasing the concentration would result in a rapid increase in voltage from an initial value of zero until a maximum point. After this maximum point, further increase in the concentration would cause a reduction in voltage which is mainly due to mixed potential losses under conditions of high crossover.

A portable DMFC system which utilizes a methanol sensor-less control method is presented in [47]. The method is discussed in detail in [48] where the cell's operating characteristics are measured to regulate the fuel concentration and to optimize the performance. It is claimed that the fuel sensor-less control algorithm is effective and is able to control the solution concentration within the range 0.5-1.3 wt% (about 0.015-0.45 M). The reliability of this method under dynamic loading conditions is experimentally verified in [49] and it is shown that the control algorithm of this method can survive during the stack continuous degradation. This control algorithm is further improved in [50]. A new load current integral function with a fixed domain is validated,

which calculates the amount of fuel consumed during the last monitoring cycle. Also, the response time is reduced in [50].

In a sensor-less method discussed in [51], it is shown that the methanol concentration in the solution fuel is a function of the open circuit voltage transient response in the methanol concentration range of 0.6-1.60 M. This method was successfully applied to a brassboard system over 20 hours of operation.

CHAPTER 3
EXPERIMENTAL METHODOLOGY

The sensor-less method is considered as one of the most desirable option to determine and control the methanol concentration in a DMFC system particularly for portable applications. In this chapter, a new sensor-less method to determine the methanol concentration in a DMFC system, including the empirical data and analysis, is explained.

Recovering the Cathode Performance Loss by Air-break

Long-term durability is one of the main challenges with regard to DMFCs [16]. In general, two types of performance losses can be identified: non-recoverable performance loss or degradation and temporary (recoverable) performance degradation. Gradual loss of active electrocatalyst surface area (anode and cathode), loss of cathode hydrophobic properties, or ruthenium crossover from the anode to the cathode through the electrolyte membrane would cause non-recoverable performance loss over long-term operation [16]. In short-term operation, loss of cathode activity due to surface oxide formation causes temporary performance degradation.

The platinum surface oxide (and/or hydroxide) leads to a decrease in the number of the free platinum sites which can inhibit the oxygen reduction reaction (ORR) on the cathode surface and reduce the cathode activity. Bringing the cathode potential down to a value that results in complete reduction of the surface platinum oxide can completely recover the cathode activity [16]. However, in a DMFC, if the cell voltage is lowered, the sluggish nature of the methanol oxidation process can lead to an increase in the anode potential which is not desirable and may induce further permanent performance degradation. An alternative method to reduce the cathode potential in DMFCs is

interrupting the air (oxygen) delivery to the cathode (air-break).During the air-break, the oxygen remaining in the cathode plenum is quickly consumed by the crossover methanol, which leads to lowering the cathode potential [16].

In a closed cathode DMFC, which was the subject of study in [16], during the air-break no more air can flow through the cathode plenum. In contrary, in an open-cathode DMFC, like the one shown in Figure 3-1, the cathode channels are open to the atmosphere. So, even during the air-break, a limited amount of air can flow through the cathode channels due to diffusion and/or natural convection due to the temperature gradient between the fuel cell stack and atmosphere. The air-break method described for a closed-cathode DMFC in [16] included four steps: a) stopping air flow to the cell, b) immediately switching cell operation to constant-current mode using the same current as the current generated by the fuel cell at the time of the switch, c) restarting airflow as soon as the cell reaches a preprogrammed low-voltage limit, d) immediately running the fuel cell in constant-voltage mode. Step (c) is fairly quick since the remaining air in the cathode plenum is quickly consumed and the cell voltage drops quickly.

By holding the cell voltage at a specified level, in case of a closed cathode DMFC, the current would quickly drop to zero since all the remaining oxygen would be quickly consumed and no more reactions could happen in the cathode. However, this would not be the case for an open cathode DMFC where even during the air-break periods a limited amount of oxygen can diffuse through the cathode channels. This can be clarified by discussing a typical load profile for an open-cathode DMFC.

Figure 3-2 shows a typical load profile for a DMFC running in a constant load (current density) mode. The red line indicates the load (current density) on the system

and the blue line shows the average cell voltage. Prior to the air-break period, the load is removed for a short period of time (10 sec in Figure 3-2) and the voltage reaches open circuit voltage (OCV). Following this step, the air flow is stopped and the cell voltage is set to a specified value (0.4 V in Figure 3-2). During the air-break, the current density initially drops rapidly and finally reaches a steady-state value. Following the air-break period, the load is removed, the cathode air flow is resumed, and the cell voltage reaches the OCV value and finally the cell continues running under a constant load. Preliminary experimental data show that the magnitude of the current density during the air-break at a constant voltage is related to the concentration of the fuel in the anode side.

Fuel Cell Testing

The fuel cell testing was conducted on an 8-cell stack built in the Fuel Cell lab at the University of North Florida. The 8-cell stack, shown in Figure 3-1, was assembled using bipolar plates such as the ones shown in Figure 3-1. A bipolar plate is a structure for distributing the reactants and collecting and distributing current. The membrane electrode assembly (MEA) was fabricated using a piece of membrane made by the UNF DMFC research group. This is a 20 μm membrane with a particular “hot-bond” adhesive coating formulation applied and laser drilled. The anode was a Johnson-Matthey electrode ELE147 which is designed to work for methanol fuel cells, with a Pt/Ru catalyst. The membrane was hot pressed with cathode and anode. The area of each MEA was 15.5 cm^2 and a total of 8 MEAs were used to build the stack.

As shown in Figure 3-3, the stack is placed in a special duct where the cathode air is delivered to the duct and flowed through the cathode channels from the bottom. The two thermocouples used to monitor the fuel solution temperature before the stack and

right after the stack are shown in Figure 3-3. The stack temperature, measured by the second thermocouple, is controlled by the amount air delivered to the duct. The cathode air mass flow controller, the heater surface and solution temperature controllers are assembled in a test station shown in Figure 3-3. In addition, the load on the stack (current or voltage mode) was controlled by a load bank integrated into the test station. The test station parameters such as the cathode flow rate, the anode solution flow rate, anode solution temperature, and the load on the system are controlled by the LabView program. The flow diagram of the test experiment configuration is shown in Figure 3-4. Note that in Figure 3-4, the test experiment configuration was such that the solution fuel was not recirculated. This configuration was used to develop a relationship between methanol concentration and the current density during the air break periods at various temperatures by using premix methanol solutions with various concentrations.

After the relationship was established, in order to evaluate the reliability and robustness of the relationship between the current density during the air-break and the solution fuel concentration, a set of test experiments was performed in a recirculating mode shown in Figure 3-5. In the recirculating mode, the methanol solution was recirculated back to the solution tank where pure methanol was added to the solution in order to maintain the concentration at a specified concentration while the solution concentration was monitored by a density type sensor (ISSYS FC-10).

Data Acquisition

The preliminary data showed that the current density during the air-break was a function of the methanol concentration in the solution fuel. Figure 3-6 shows sample data taken with 0.9 M fuel solution, stack temperature of 50 ^{o}C, and a constant voltage of 0.4 V during the air-break. The air-break period is clearly shown and defined in Figure

3-6. Note that prior to and right after the air break, the stack undergoes a “no load’’ period with the air present. After an initial rise, the current density falls down and reaches a steady-state value. This steady-state value is dependent on the methanol concentration in the fuel as shown in Figure 3-7.

Figure 3-7 shows the sample data for a range of solution concentrations of 0.3-1.5 M at a stack operating temperature of 50 ^{o}C and 0.4 V/cell during the air-break. Clearly, the current density during the air-break at a constant voltage is inversely related to the methanol concentration in the fuel solution. This relationship could be a function of the operating temperature, the voltage during the air-break, or the operating time of the stack. The data shown Figure 3-7 can be presented in the form shown in Figure 3-8, where current densities at three particular moments of the air-break period are graphed versus the solution fuel concentration.

The conducted experiments for this work were performed in two categories. In the first category, the experiments were focused on studying the effective parameters on the relationship between the current density during the air-break and the solution fuel concentration. These parameters were including the following: the set voltage during the air-break, the operating temperature, and the operating time of the stack. Studying the effect of the set voltage during the air-break helped to determine which set voltage resulted in better resolution. A series of test experiments was conducted for a range of premixed methanol solution of 0.3-1.5 M and air-break voltage of 0.4, 0.3, 0.2, 0.1, and 0.05 V/cell. In all experiments, the stack was operated on a no-load mode (OCV) for two periods, one prior to the air-break and one right after the air-break ends, with each period lasting 15 seconds. By investigating the effect of the operating temperature, an

empirical model was developed which can determine the methanol concentration for an operating temperature range of 45-55 ^{o}C and methanol concentration range of 0.3-1.5 M. Also, since the performance of DMFCs is subjected to degradation over long term operation, the validity of this method was examined over 1700 hours of operation.

The second category of the experiments was dedicated to study the reliability of this method through statistical analysis and also in comparison with a methanol concentration sensor. The repeatability of the data was studied over 50 consecutive load cycles for a given operating temperature and solution concentration. Finally, the empirical model was validated in comparison with a methanol concentration sensor over an operating temperature range of 45-55 ^{o}C and methanol concentration range of 0.3-1.5 M.

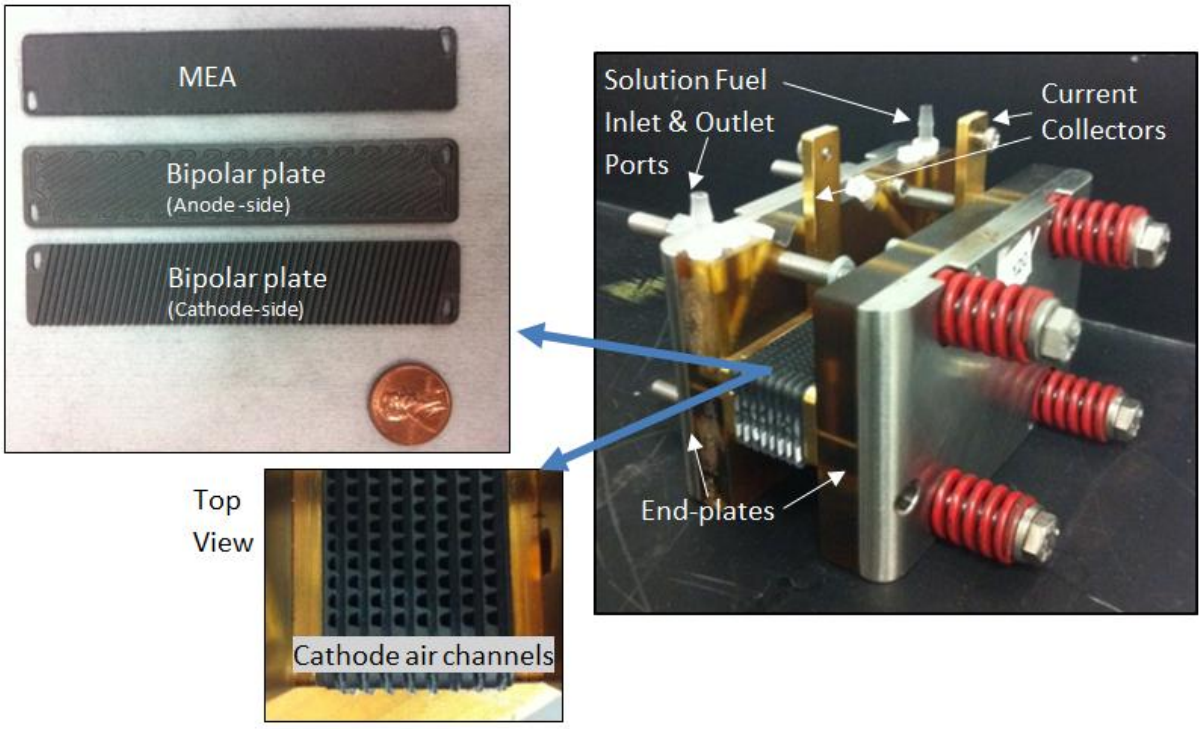

Figure 3-1. An open-cathode DMFC and its components. Courtesy of Amir Shoraka.

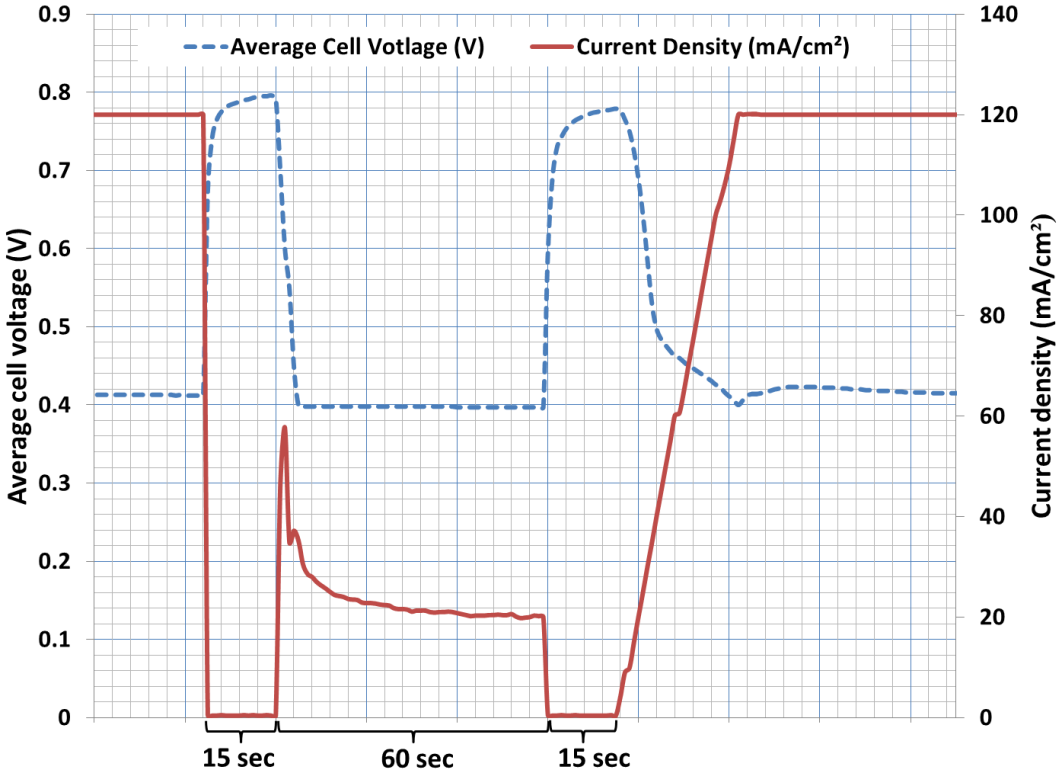

Figure 3-2. A typical load profile for a DMFC.

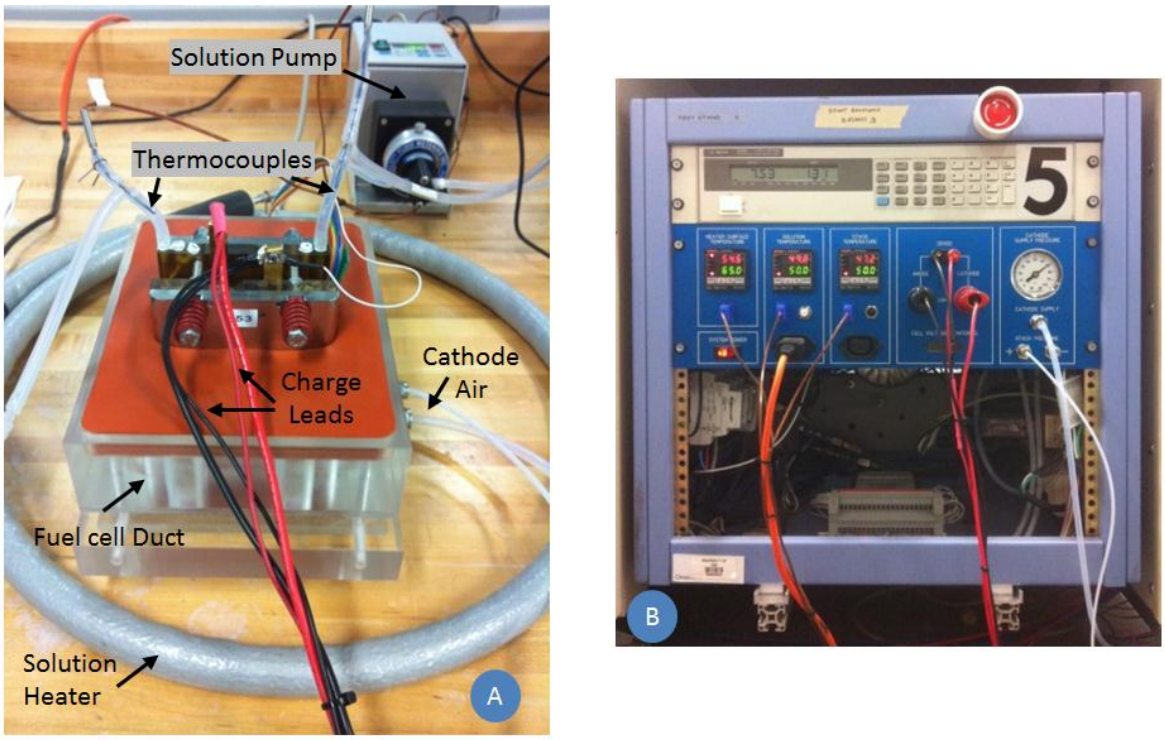

Figure 3-3. A) Test rig components B) Test station. Courtesy of Amir Shoraka.

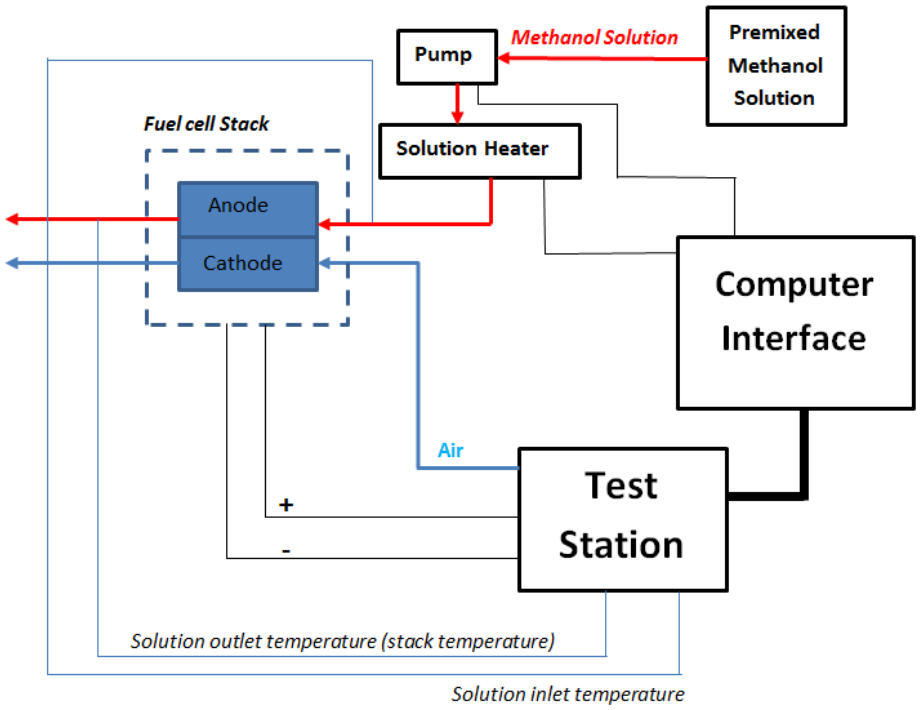

Figure 3-4. Test experiment flow diagram (Flow through mode).

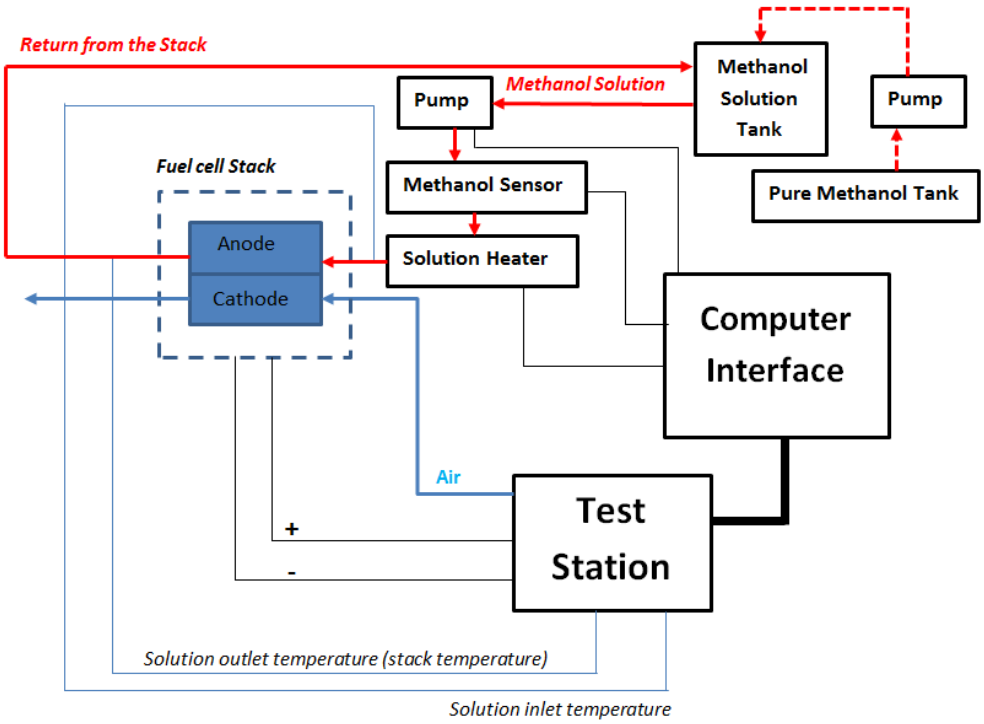

Figure 3-5. Test experiment flow diagram (Recirculating mode).

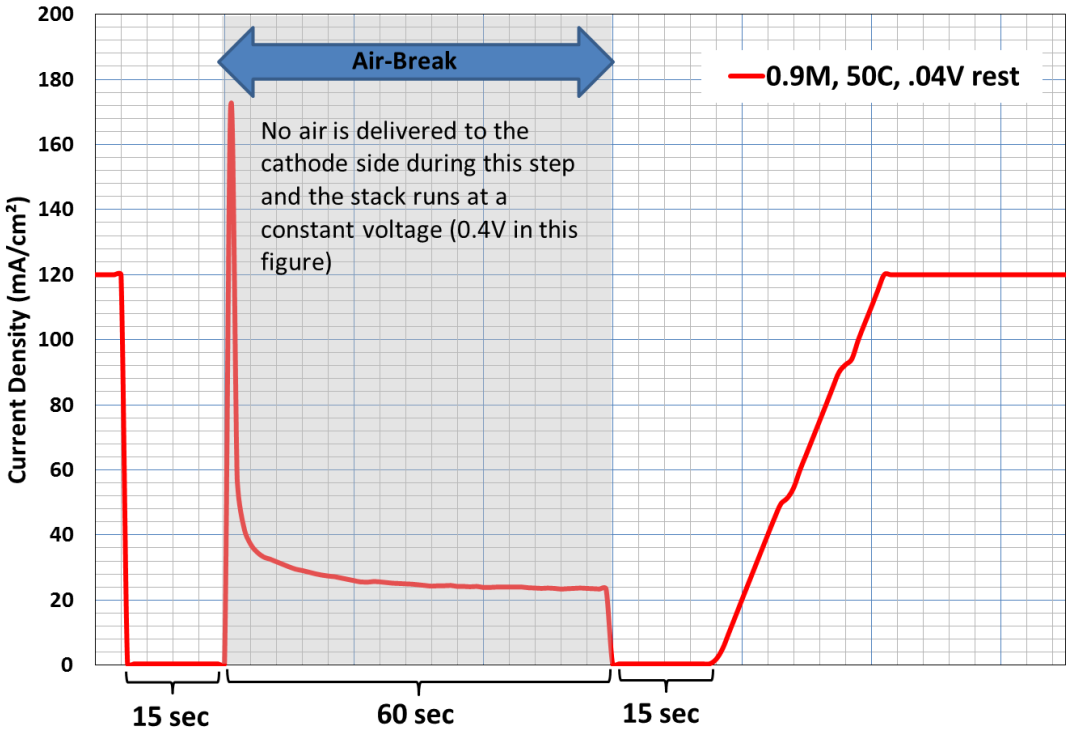

Figure 3-6. A sample data taken at 0.9M fuel solution, 50C, and a constant voltage of 0.4V during the air-break.

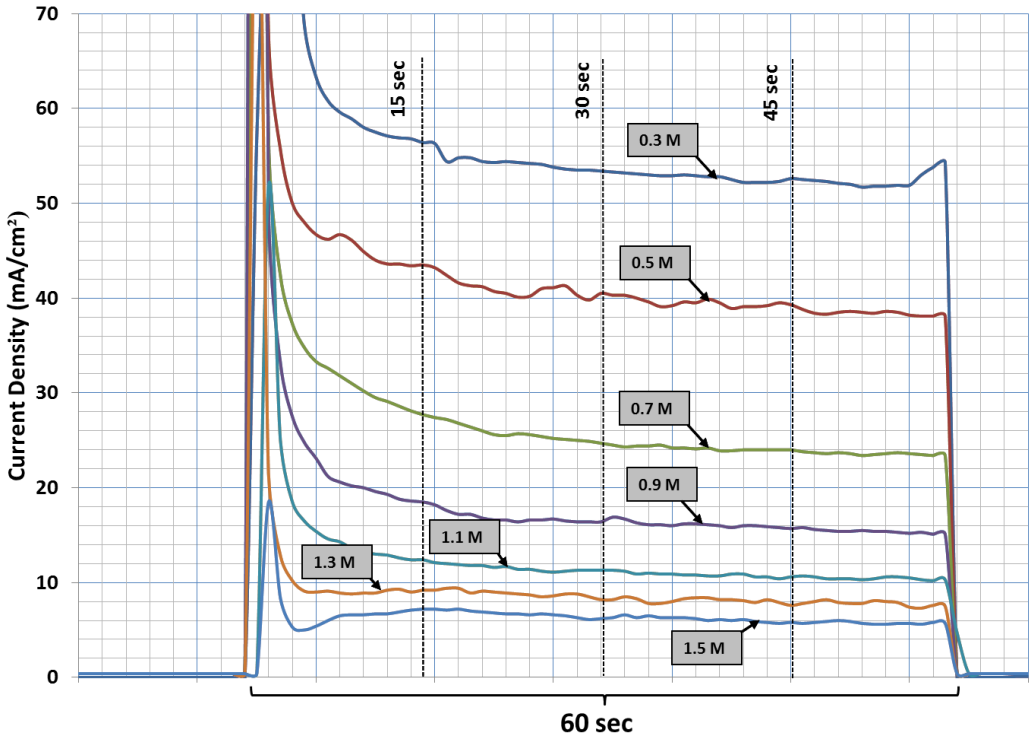

Figure 3-7. Sample data for various fuel solutions concentrations at 50 ºC and 0.4 V during the air-break.

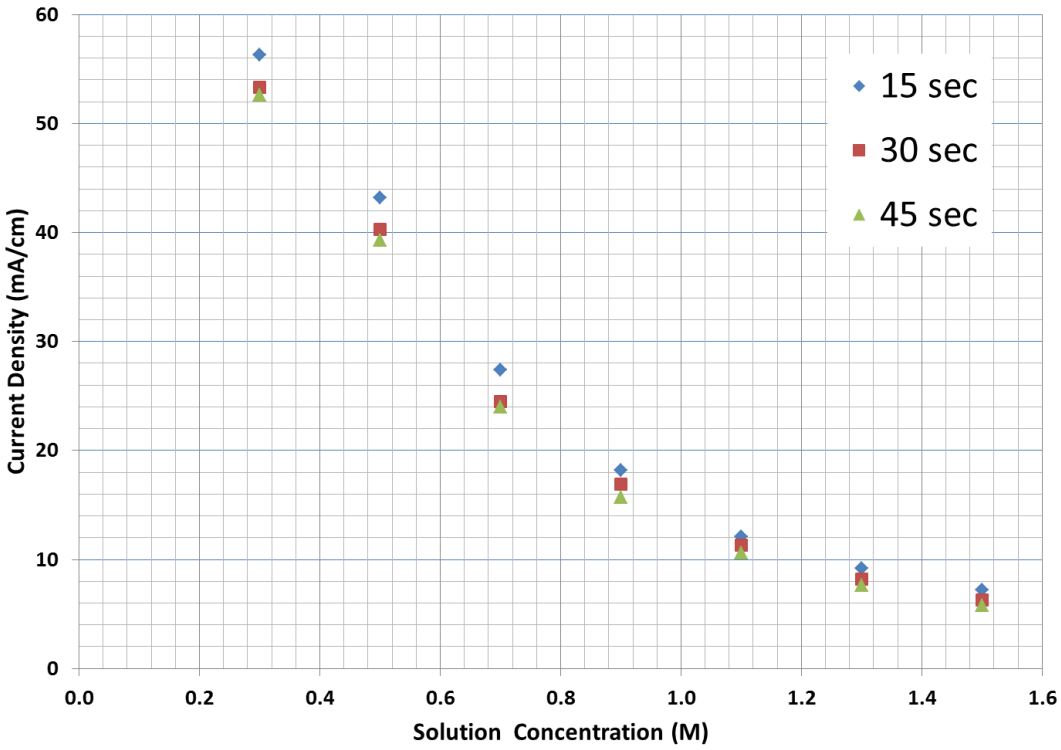

Figure 3-8. Current density during the air-break vs. solution fuel concentration at 50°C and 0.4V rest.

CHAPTER 4
RESULTS AND DISCUSSION

In this chapter, the tests results are shown and the relation between the fuel concentration and the current during the air-break is discussed. In addition, the effects of the voltage during the air-break, the stack temperature, the operating hours of the stack are discussed.

The Effect of Voltage during the Air-Break

Figure 4-1 shows the data taken for various premixed solution concentrations at a stack operation temperature of 50 ^{o}C and set voltage of 0.4 V/cell. For the purpose of comparison in this section, the curves are constructed at 45th of a 60-second air-break (45 seconds after the air delivery was stopped and a constant voltage load of 0.4 V/cell was imposed on the stack).

The current density during the air-break is inversely related to the fuel solution concentration. The reason for such a behavior can be attributed the higher rate of methanol crossover at higher solution concentrations. Note that the methanol crossover is driven by diffusion phenomenon and hence, higher concentration in the anode side would increase the rate of methanol crossover. During the air-break, a limited amount of oxygen can diffuse to the cathode channels during the air-break which can be consumed for either the cathode oxygen reduction reaction or can react with the crossover methanol within the cathode catalyst layer. The higher the solution fuel concentration results in a higher rate of methanol crossover and consequently more oxygen would be consumed for the methanol oxidation reaction. This means less oxygen would be available for the cathode oxygen reduction reaction and as the result,

lower current density would be observed. This is explained in detail and proven in Appendix A.

Figure 4-2 shows the effect of reducing the voltage from 0.4 V/cell to 0.3 V/cell during the air-break period where the curve is shifted upward. This can be explained by considering the polarization curve for a DMFC (Figure 1-2), where generally decreasing the voltage results in a higher current density. In Figure 4-3, the result of the experiments for a range of air-break voltages is shown. In general, the current density during the air-break increases as the voltage is set to a lower value during the air-break, which can be explained by considering the polarization curve.

Within the first portion of the polarization curve (Figure 1-2), where the activation losses are the dominant type of performance losses, decreasing the voltage does not significantly increase the current density, so the increase in the current density is not significant as the air-break voltage is decreased from 0.4V to 0.3V or even 0.2 V. However, within the second region of the polarization curve, where the ohmic losses are dominant, a small decrease in the voltage can significantly increase the current density and this could explain the significant increase in the current density from 0.2 V to 0.1 V or 0.05 V during the air break. In case of the very low solution concentration such as 0.3 M, the current density does not increase significantly by reducing the voltage lower than 0.1 V during the air-break which can be caused by the concentration losses which is dominant in third region of the polarization curve (Figure 1-2).

Considering the curves for various voltages during the air-break, the curves related to the low voltages such as 0.1 and 0.05V/cell during the air-break have less

resolution when compared with the curves related to the higher voltages during the rest such as 0.4, 0.3, or 0.2V/cell during the air-break.

The Effect of the Stack Operating Temperature

The effect of the stack operating temperature on the current density during the air-break was studied by performing a set of experiments over a stack operating temperature range of 45 - 55 ^{o}C. Figure 4-4 shows the result of a set of experiments conducted at 0.4 V/cell during the air-break. Generally, as the operating temperature increases the current density during the air-break decreases for a particular solution concentration. The reason for this could be mainly attributed to higher rates of methanol crossover at higher temperatures. Since methanol crossover is a diffusion phenomenon, it is highly temperature dependent. The effect of the temperature increase is less pronounced at very low concentrations such as 0.3 M due to the extremely low methanol concentration at the anode catalyst and membrane interface (concentration loss part of the polarization curve).

The Effect of the Stack Operating Hours

The performance degradation is one of the challenges about of DMFCs. This work is not intended to discuss DMFCs' performance degradation issue; however, since the method introduced in this thesis is dependent on the performance of DMFC during the air-break, it is necessarily to investigate the effect of the operating hours of the DMFC on this method. During the time that the 8-cell stack was not being used in any specific experiment, it was operating at a typical constant load of 120 mA/cm^2 and operating temperature of 50 ^{o}C with 60-second air-break periods every 10 minutes of operation. By implementing this strategy, investigation of the effect of the operating time was possible. The performance of the 8-cell stack was measured at several specified

times over a range of solution concentrations of 0.5-1.5 M. The result is shown in Figure 4-9.

There is a significant change between the data taken after 200 hours operation hours compared with the data taken after 650 hours of operation. It is possible that the DMFC have an initial degradation during the first few hundred hours of operation followed by a much slower rate of degradation. This could explain why there is not a significant difference between the data taken after 650 hours of operation in comparison with the data taken after 1150 hours of operation or the data taken after 1650 hours of operation. Since the performance degradation is a complicated issue, affected by various factors including the MEA structure, catalyst, and even the load profile, a comprehensive set of test experiments including several DMFC stacks must be conducted prior to expressing any certain conclusions regarding the effect of the operating hours of the fuel cell on this method. This is beyond the scope of this work. However, Figure 4-9 shows that the effect of the operating hours is not significant after the first few hundred hours of the stack operation hours for this type of DMFC and this stack in particular.

Statistical Analysis

Before this method can be used as a methanol concentration measurement technique, it is important to know the measurements' repeatability. A comprehensive set of statistical experiments was performed at stack operating temperature of 50 ^{o}C and the air-break voltage of 0.4 V/cell for a range of premixed methanol solutions of 0.3-1.5 M. The statistical experiment for each solution concentration included 50 repetitive cycles and each cycle was comprised of four steps: 1) 300 seconds running at a constant load of 120 mA/cm at a stack temperature of 50 ^{o}C that is controlled by the

cathode air flow, 2) 15 seconds running at no-load (OCV) with a cathode flow rate of 4 SLPM/cell, 3) 60 seconds of running at a constant voltage of 0.4 V/cell (air-break), and 4) 15 seconds running at no load (OCV) with a cathode flow rate of 4 SLPM/cell. The purpose of this experiment was to compare the performance of the stack during the air-break periods of 50 consecutive cycles. A sample of the statistical experiment conducted for a premixed fuel solution of 0.5 M is shown in Figure 4-6.

The circles in Figure 4-6 show the current density during the air-break periods. In Figure 4-7 the performance of the stack during 50 consecutive air-break periods is shown. Each cross sign indicates one cycle and the black circles represent the average of the performance values at any given second of a 60-second air-break.

The result of the statistical experiment, conducted for a range of premixed solution concentrations of 0.3-1.5 M, is shown in Figure 4-8. Table 4-1 shows the average (m) and standard deviation (σ) values at 15^{th}, 30^{th}, and 45^{th} second of the air-break periods. It is shown in Table B-1 that the data has a normal distribution for 50 samples at any given second. Statistically, it means there is no systematic variation in the data and the probability that a random measurement falls in the range of [m- σ, m+ σ] is roughly 0.65 and the probability that a random measurement fall in the range of [m- 2σ, m+ 2σ] is roughly 0.96.

The data shown in Table 4-1 is presented in the form of three plots which each shows the current density as a function of solution concentration at a particular time after the start of the air-break period. The error bars in Figure 4-9, Figure 4-10, and Figure 4-11 show the range of the data for a particular concentration. Considering the curves shown in Figure 4-9, Figure 4-10, and Figure 4-11, it could be concluded that,

statistically, there is no significant advantage for choosing any particular curve over the others.

Comparing the Method with a Methanol Concentration Sensor

The reliability of this method was examined by comparing the result of this method with the measurements of a methanol concentration sensor. In order to do so, a test set up shown in Figure 3-5 was prepared. The methanol sensor used for this experiment was an ISSYS FC-10, shown in Figure 4-12, which is suitable for methanol concentration range of 0-30%wt and temperature range of 0-70^{o}C.

The methanol sensor was able to continuously measure and monitors the solution concentration, however, the method introduced in this work was only able to determine the solution concentration during the air-break periods. So, in order to compare the results from the sensor and this method, the calculated methanol concentrations based on the current density at three particular moments during the air-break (the 15th, the 30th, and the 45th second of a 60-second air-break) were compared to the solution concentration measured by the sensor at the beginning of the air-break period. The experiment was conducted at a range of solution concentration of 0.4-1.5M and operating temperatures of 45-55 ^{o}C. In Figure 4-13, the sensor reading, the calculated concentration, and the difference between the method and the sensor readings at 50 ^{o}C is shown. The calculated methanol concentration is based on the current density at the 15th second of the air-break period. The average difference over a range of methanol concentration of 0.3-1.5 M at 50 ^{o}C is 0.067 M. However, the average difference associated with the lower methanol concentration region, 0.3-0.9 M, is 0.061 M and for the higher methanol concentration region, 0.9-1.5 M, is 0.074 M. The slightly lower

difference could be due to the better resolution (steeper slope) in the lower concentration region of the curve shown in Figure 4-1.

The results of the experiments conducted over a range of temperature of 45-50 ^{o}C and at the 15th, 30th, and 45th second of the air-break period are shown in Figure 4-14, Figure 4-15, and Figure 4-16, respectively. As mentioned earlier, this method is not able to continuously determine the methanol concentration and the points shown in Figure 4-14, Figure 4-15, and Figure 4-16 represent the calculated solution concentration at particular moments during a 60-second air-break period.

The average difference associated with different parts of the above three figures are shown in Table 4-2. In general, the average difference is smaller for the low methanol concentration region, 0.3-0.9 M. Also, it can be concluded that there is no significant advantage of calculating the methanol concentration based on the current density at 30th or 45th second of the air-break period in comparison with that based on the current density at the 15th second of the air-break period. This means an air-break period as short as 15 seconds can be sufficient for the purpose of implementing this method. During the air-break, the power generated by the DMFC is significantly lower than normal operation and hence long air-break periods are not desirable.

The average differences for the calculation based on the current density at the 15th, 30th, and 45th second of the air-break period are 0.066 M, 0.069 M, and 0.068 M, respectively. In general, the result of the comparison test experiment looks promising particularly in terms of the difference in determining the methanol concentration.

In this chapter the effect of several parameters such as the operating temperature and the operating hours of the stack on this method were discussed. The effect of the

operating temperature was considered in the calculations, but the effect of the stack life time or the performance degradation on this method can be revealed only by conducting a set of comprehensive test experiments over various types of MEAs which is beyond the scope of this thesis. However, the results shown in this chapter certainly show that the methanol concentration in an open-cathode DMFC can be determined by measuring the current density during the air-break and this method has potential to be used in a DMFC system to determine the methanol concentration in the fuel solution.

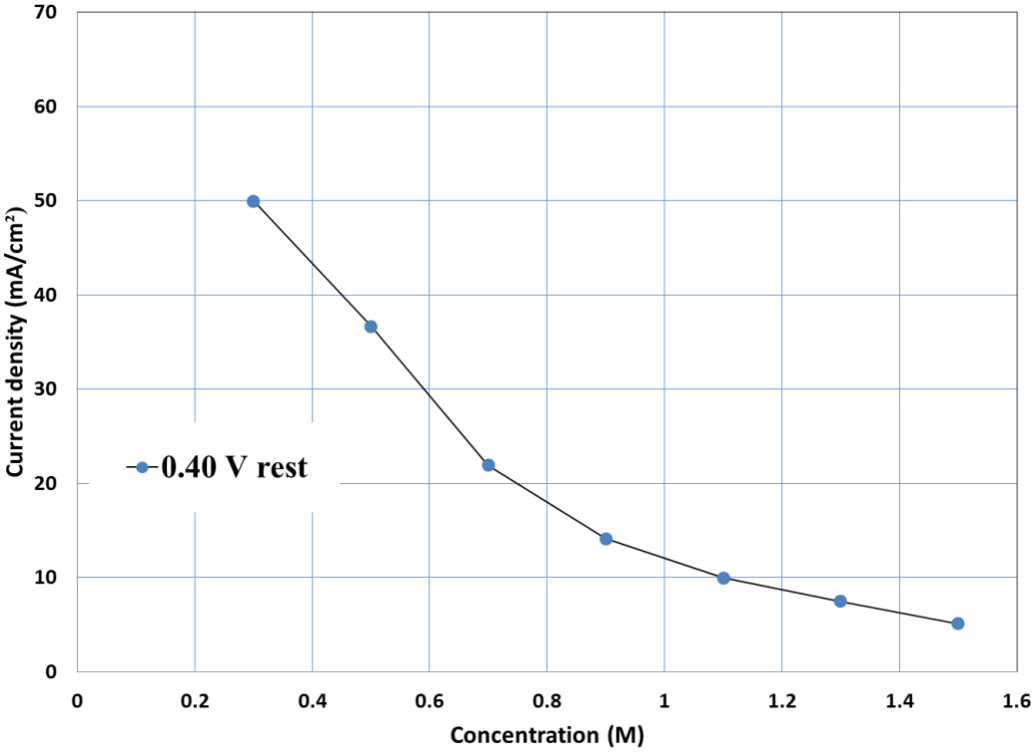

Figure 4-1. Current density during the air-break vs. solution concentration at 50 °C and 0.4V rest.

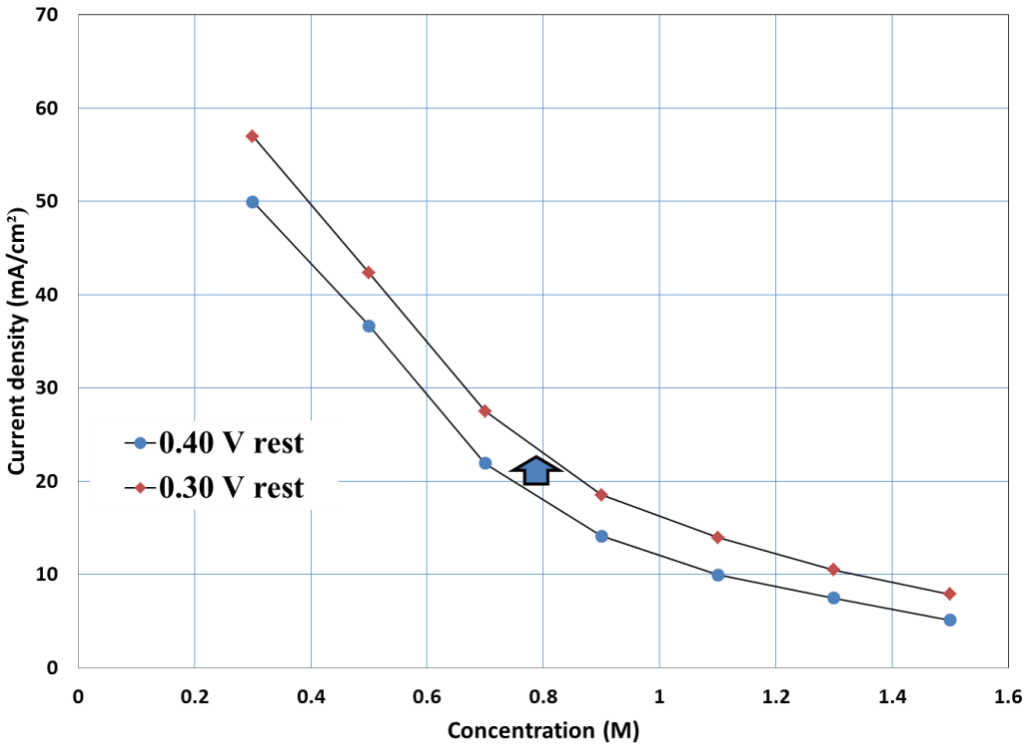

Figure 4-2. Comparing the current density during the air-break vs. solution concentration at 50 °C, for 0.4V rest and 0.3V rest.

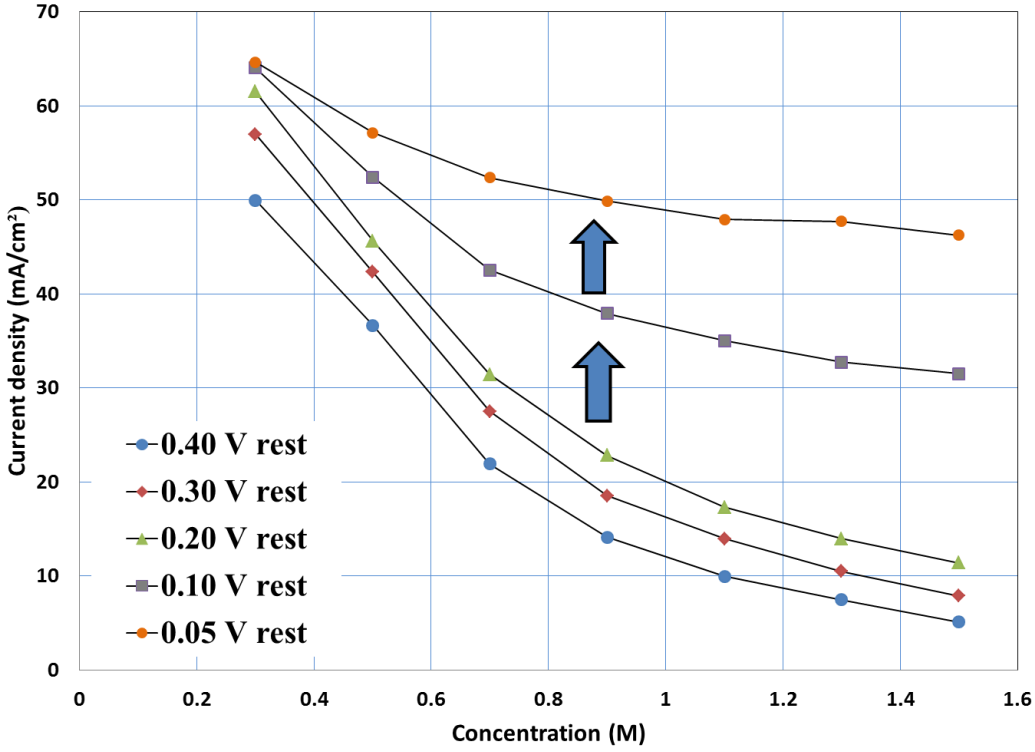

Figure 4-3. Comparing the current density during the air-break vs. solution concentration at 50 °C, for 0.4, 0.3, 0.2, 0.1, and 0.05 V/cell during the air-break.

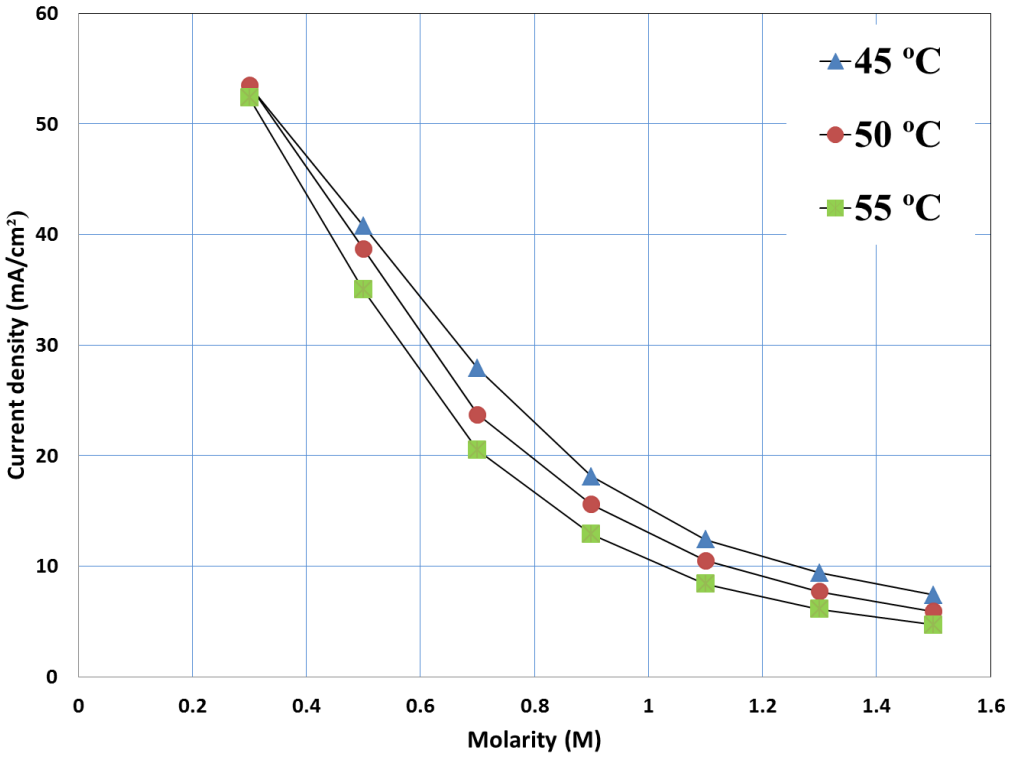

Figure 4-4. Effect of the stack operating temperature on the current density during the air-break at 0.4V/cell rest.

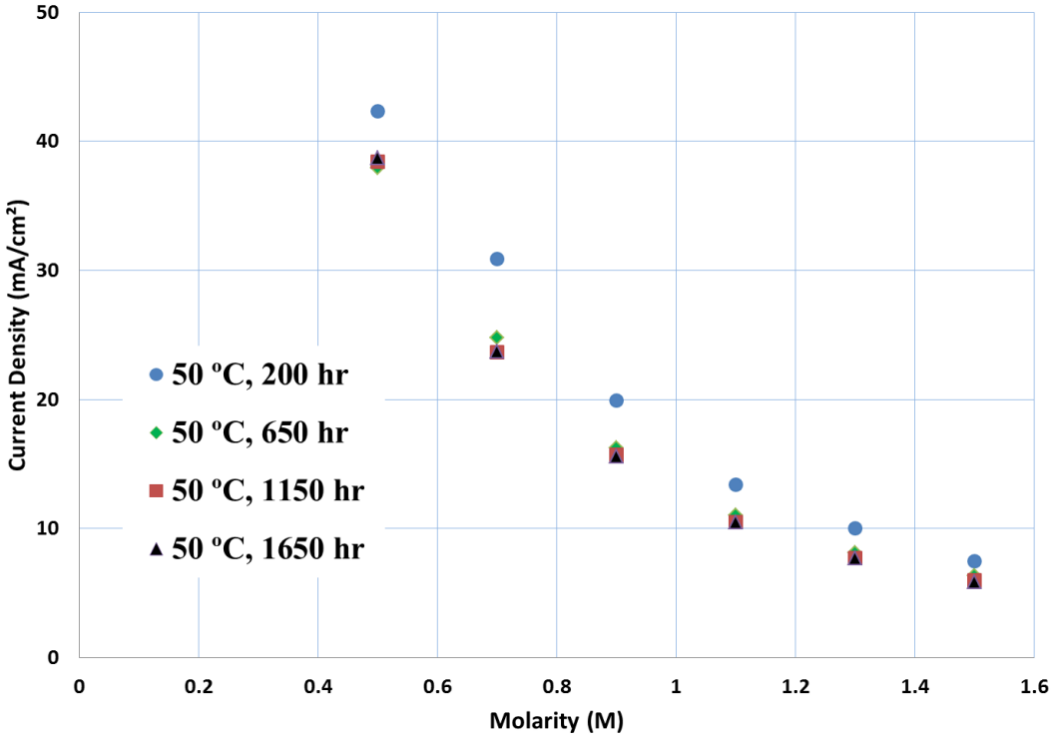

Figure 4-5. The current density during the air-break vs. concentration at the operating hours of 200, 650, 1150, and 1650 hour.

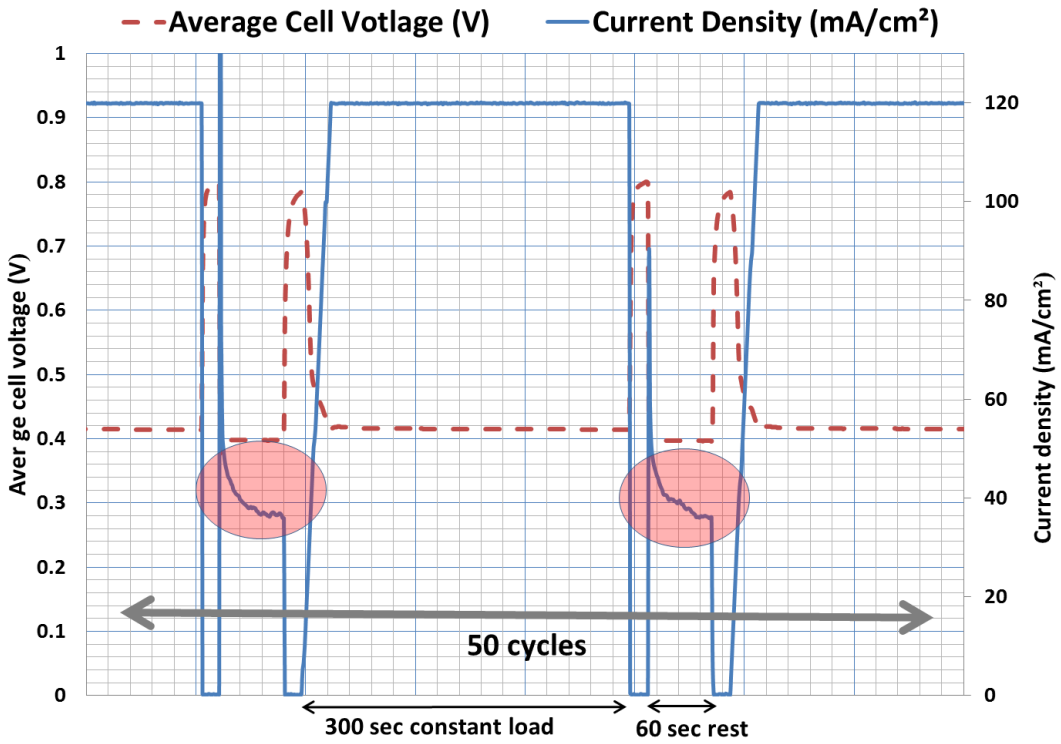

Figure 4-6. Sample statistical experiment conducted for 0.5 M solution.

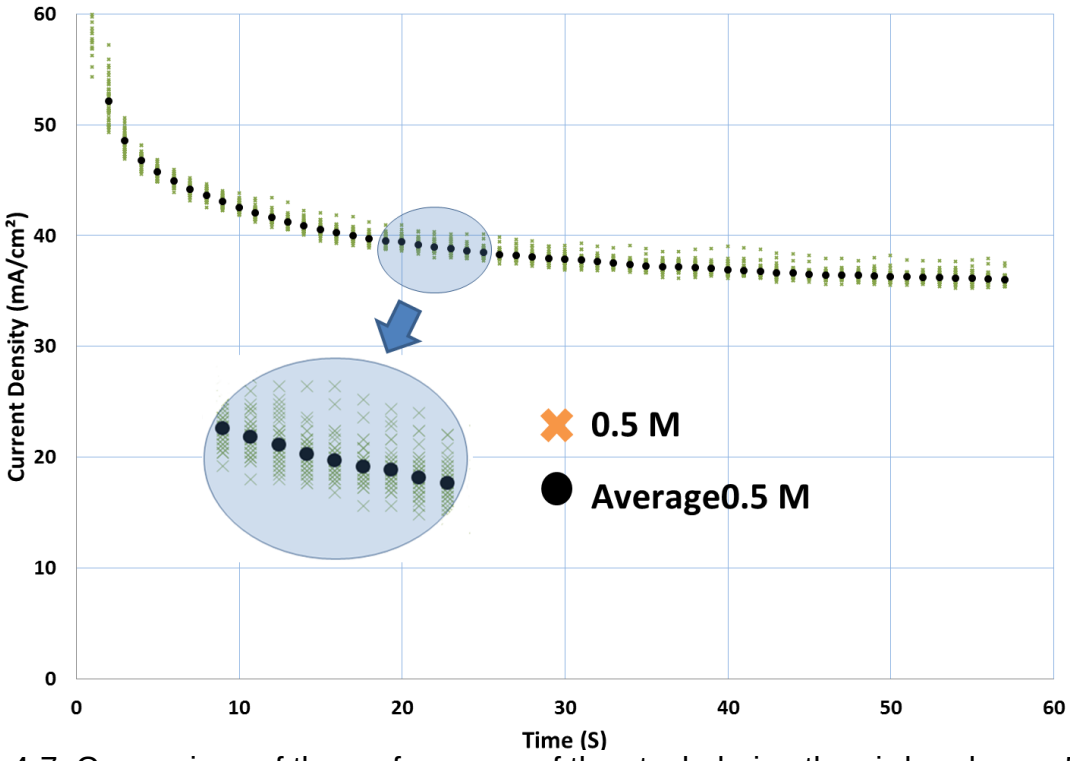

Figure 4-7. Comparison of the performance of the stack during the air-break over 50 consecutive load cycle.

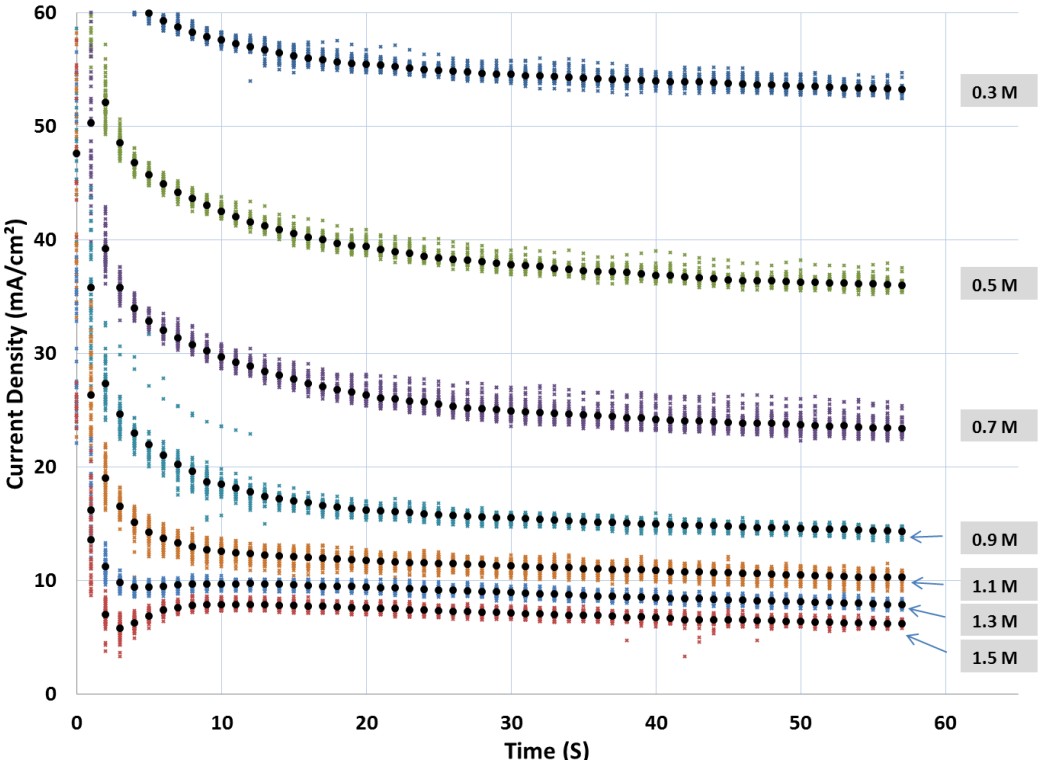

Figure 4-8. Comparison of the statistical experiment for the premixed solution range of 0.3-1.5 M, 50ºC stack operation temperature, 0.4 V/cell rest (50 cycles.

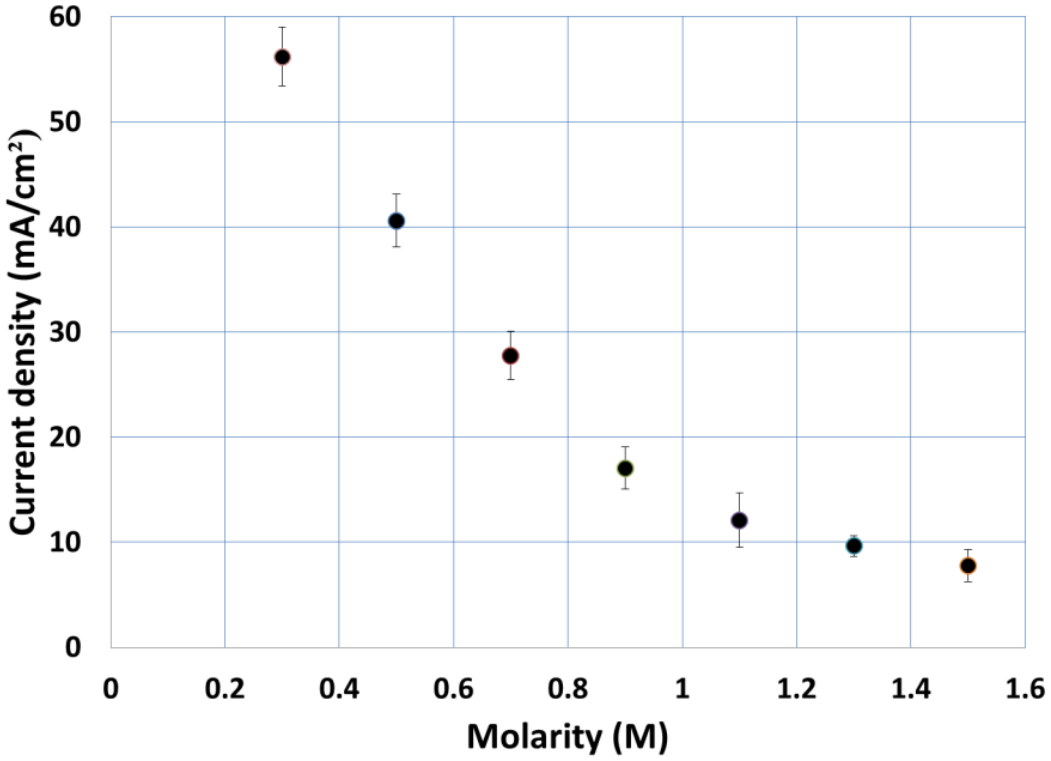

Figure 4-9. The average values (black dots) and the range of the data (error bars) for a range of concentration of 0.3-1.5M and 50°C at 15th second of the air-break period.

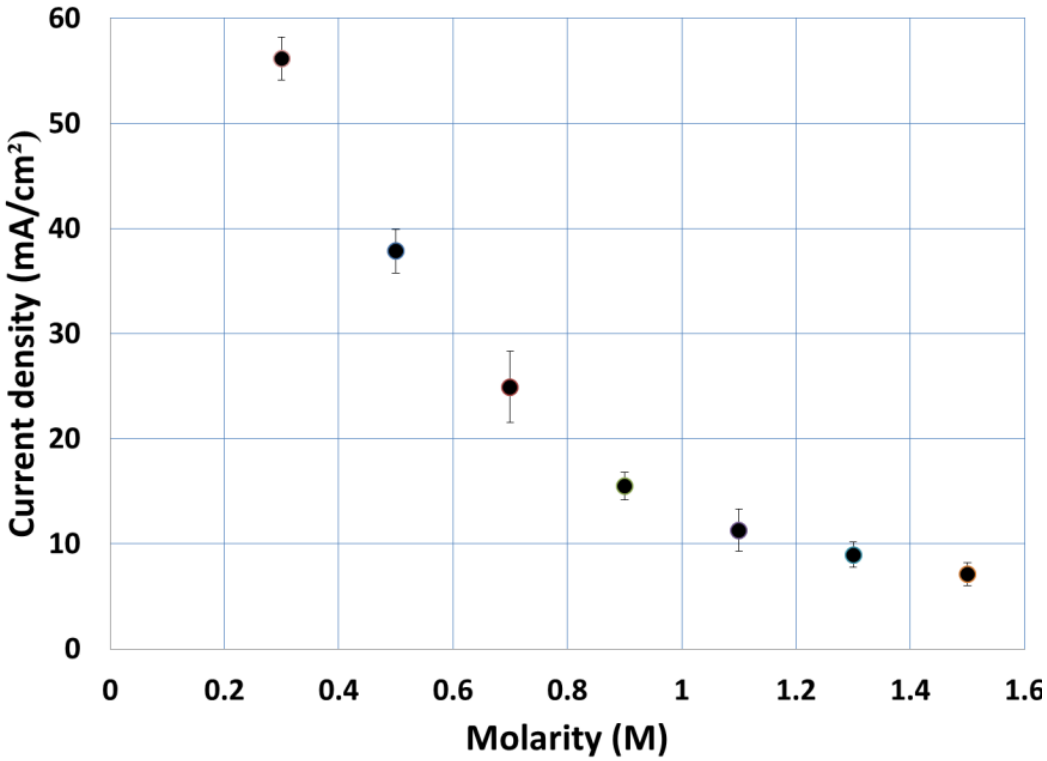

Figure 4-10. The average values (black dots) and the range of the data (error bars) for a range of concentration of 0.3-1.5M and 50°C at 30th second of the air-break period.

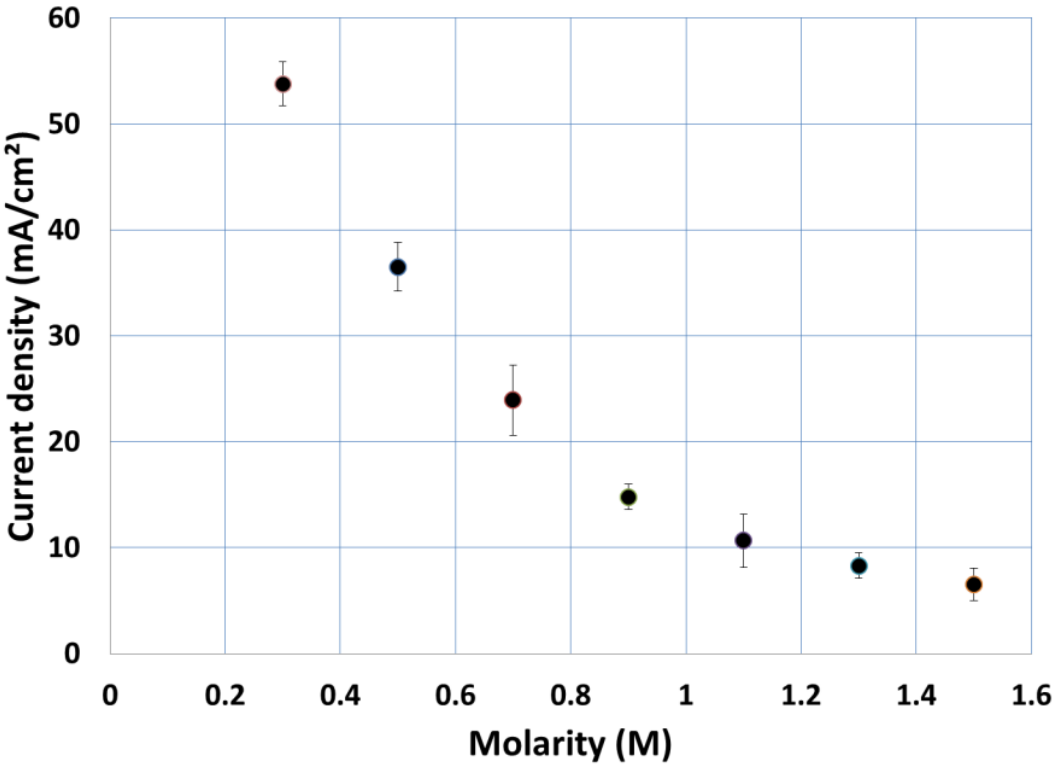

Figure 4-11. The average values (black dots) and the range of the data (error bars) for a range of concentration of 0.3-1.5M and 50°C at 45th second of the air-break period.

Figure 4-12. ISSYS FC-10 methanol sensor. Courtesy of Amir Shoraka.

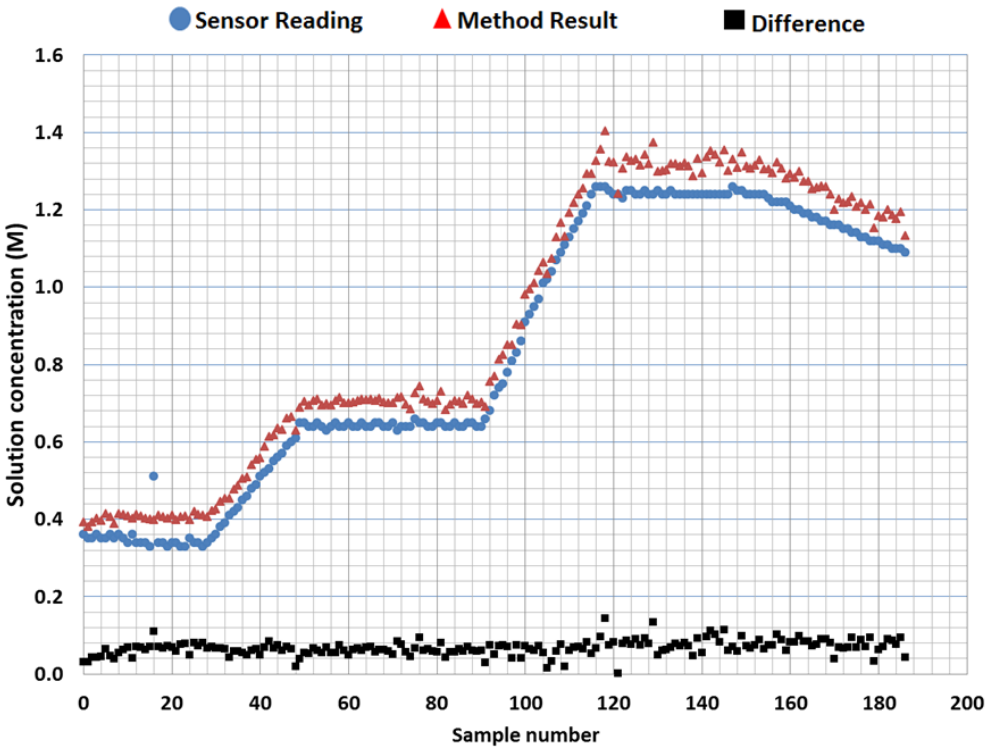

Figure 4-13. Measured (sensor reading) and calculated methanol concentration at 15th second of the air-break period and 50 ^{o}C.

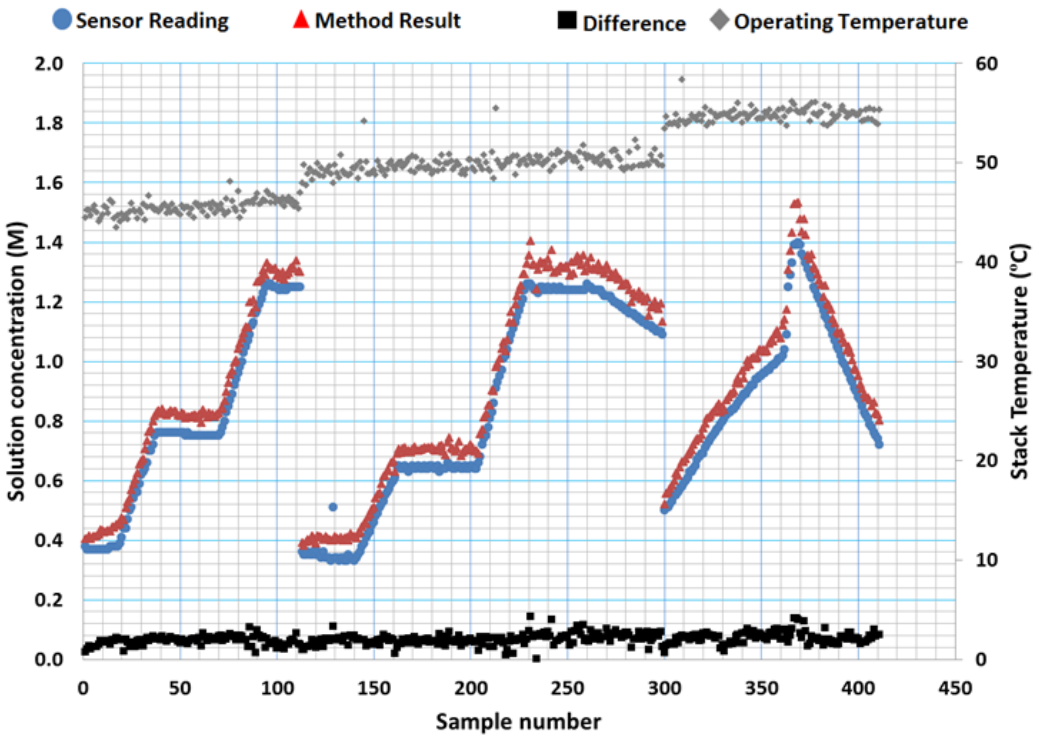

Figure 4-14. Measured and calculated solution concentration at various operating temperatures, 0.4V rest, 15th second of the air-break period.

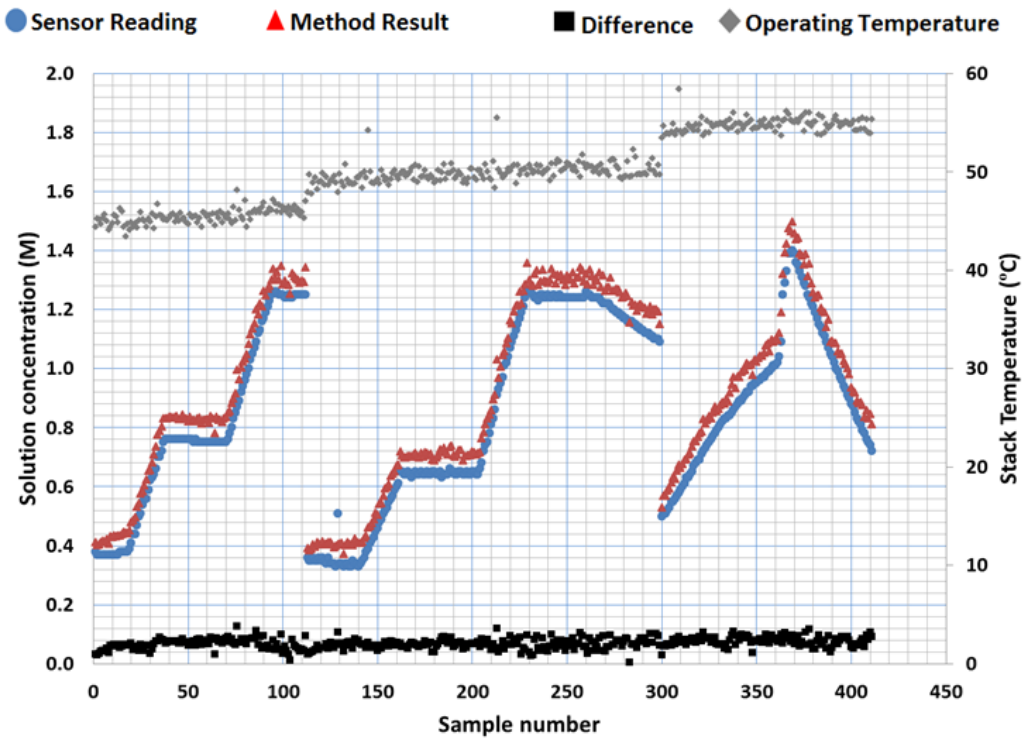

Figure 4-15. Measured and calculated solution concentration at various operating temperatures, 0.4V rest, 30th second of the air-break period.

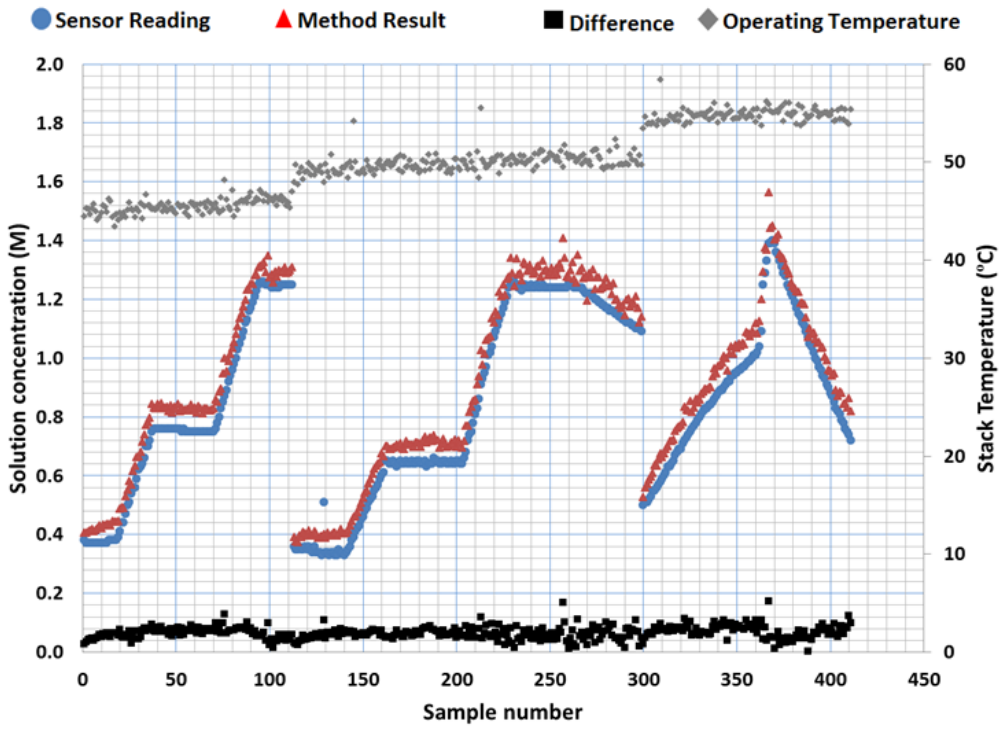

Figure 4-16. Measured and calculated solution concentration at various operating temperatures, 0.4V rest, 45th second of the air-break period.

Table 4-1. The average value and the standard deviation at the 15th, 30th , and 45th second of the air-break period for various solution concentrations at 50 °C and 0.4 V/cell rest.

Solution concentration (M)	15th second average current density (mA/cm²)	30th second average current density (mA/cm²)	45th second average current density (mA/cm²)	15th second standard deviation	30th second standard deviation	45th second standard deviation
0.3	56.17	54.56	53.79	0.574	0.397	0.447
0.5	40.60	37.84	36.49	0.453	0.404	0.390
0.7	27.76	24.93	23.92	0.564	0.709	0.722
0.9	17.04	15.51	14.80	0.403	0.316	0.338
1.1	12.09	11.27	10.65	0.525	0.427	0.468
1.3	9.63	8.94	8.30	0.258	0.291	0.282
1.5	7.77	7.13	6.53	0.288	0.267	0.300

Table 4-2. The average difference of the calculated methanol concentration in comparison with the sensor readings.

Calculation based on	45 ºC		50 ºC		55 ºC	
	0.3-0.9 M	0.9-1.5 M	0.3-0.9 M	0.9-1.5 M	0.3-0.9 M	0.9-1.5 M
15th second	0.061 M	0.063 M	0.061 M	0.074 M	0.067 M	0.080 M
30th second	0.065 M	0.067 M	0.064 M	0.068 M	0.076 M	0.079 M
45th second	0.066 M	0.065 M	0.062 M	0.061 M	0.077 M	0.068 M

CHAPTER 5
CONCLUSIONS

The performance current density of an open-cathode DMFC during the air-break period at a constant voltage is inversely related to the methanol concentration of the anode fuel solution (Figure 3-7) and this relationship is more distinct in the lower concentration region (less than 0.9M), (Figure 4-1). The methanol concentration in the fuel solution was determined by developing a relationship between the performance of the stack during the air break and the methanol concentration in the fuel solution over a range of methanol concentrations of 0.3-1.5 M and a range of stack operating temperatures of 45-55 ^{o}C, which resulted in an average of difference of 0.068 M with respect to the measurements of a methanol sensor. It is believed that this error is acceptable for a methanol concentration method.

The effect of stack operating temperature, voltage during the air-break, and life time of the stack on this method were studied. The current density during the air-break was found to be inversely related to the stack operating temperature (Figure 4-4). This is mainly attributed to the higher rate of methanol crossover at higher operating temperatures. Reducing the air-break voltage generally increased the current density during the air-break at a particular concentration (Figure 4-3). Regarding the effect of the stack operating time, a solid conclusion may not be expressed at this point, since a comprehensive set of experiments including several fuel cell stacks is required; however, for the particular stack used in this work, the current density-concentration curve remained fairly consistent for stack operating time greater than 650 hours (Figure 4-5). Moreover, the consistency of the performance during the air-break periods was statistically analyzed over a range of methanol concentrations of 0.3-1.5 M and over 50

consecutive air-break periods and It was found that the measurements had a normal distribution and there was no systematic variation in the measurements for a particular concentration.

This work discussed a new method to determine the methanol concentration in an open-cathode DMFC system that has potential to be used as a methanol sensing strategy because of its unique features. This method does not require any auxiliary device since it is using the readily available data during the air-break period, which is a conventional strategy to recover the cathode potential. Also, this method could be particularly suited for use as a secondary sensor by which the performance of the primary methanol sensor can be examined.

Future work could focus on the effect of the MEA structure on methanol crossover. This could include the thickness of the membrane which is inversely related to the methanol crossover or the structure of the cathode side, particularly the barrier layer which affects the oxygen diffusivity to the cathode catalyst layer. These two could significantly influence the current density during the air-break. Also, better understanding of the effect of the stack life time on this method must be a priority in the future works. In addition the reproducibility of this method can be evaluated by conducting identical test experiments on multiple stacks. The effect of the ambient air properties such as pressure and temperature, and the stack orientation need to be studied as well.

APPENDIX A
A DISCUSSION ABOUT THE SHAPE OF THE CURVES

The purpose of this chapter is to discuss the effective parameters that shape the air-break current density – concentration curve and then experimentally proving the discussed parameters. Also, measuring the diffusion-limited methanol oxidation current as a method to measure the methanol diffusion coefficient in the membrane will be discussed.

Factors Affecting the Shape of the Curves

The first and possibly most important aspect of the curves shown in Figure 4-9 is that the current density during the air-break is inversely related to the methanol concentration in the fuel. However, this inverse relationship is more distinct in the lower methanol concentration region (less than 0.9 M). The reason for this trend can be attributed to the fact the rate of the methanol crossover is a strong function of the methanol concentration in the anode side; hence, an increase in the methanol concentration in the solution fuel increases the rate of the methanol crossover to the cathode side. During the air-break in an open cathode DMFC, a limited amount of air flow exists in the cathode channels mainly due to the buoyancy effect and the temperature gradient between the fuel cell stack and environment. The oxygen carried in the cathode channel by the limited air flow is mainly consumed in two different reactions: the cathode reaction (ORR) and methanol cross over oxidation reaction (methanol combustion) at the presence of the cathode catalyst. The higher rates of the methanol cross over means that a larger portion of the limited available oxygen is consumed for the methanol oxidation reaction and less oxygen is left for the cathode reaction and consequently less current density is observed. The methanol oxidation

reaction is not advantageous in terms of current generation and it is a waste of fuel. However, the fact that the methanol crossover is a function of the methanol concentration in the anode fuel is the main reason that the current density during the air-break is a function of the solution fuel concentration.

Methanol Crossover Modeling

A simple methanol crossover model based on Fick's law of diffusion was created. Fick's law [52] of diffusion defined as:

$$J = -D \frac{dC}{dx} \quad \text{(A-1)}$$

where J (mol/m^2.s) is the diffusion flux, D (m^2 /s) is diffusion coefficient, and dC/dx (mol/m^3) is the concentration gradient. The diffusion coefficient of methanol through the MEA can be calculated by measuring the diffusion limited methanol oxidation current. In order to conduct this experiment, the fuel cell cathode is purged with nitrogen and the fuel cell is connected to a power supply.

This means that the 8-cell stack is not further operating as a galvanic cell which produces electricity; in fact, the 8-cell stack operates as a electrolytic cell in which methanol diffuses through the membrane and is oxidized within the cathode catalyst layer. The protons and the electrons liberated in the methanol oxidation reaction react within the anode catalyst layer which results in hydrogen formation in the anode side. The details of this experiment are shown in Figure A-1. The experiment starts with setting the power supply voltage to zero. By gradually increasing the voltage controlled by a power supply, the current eventually starts increasing which is the result of the methanol oxidation in the cathode and hydrogen evolution in the anode side. After a certain point, increases in the supplied voltage do not increase the current [53]. This maximum current value is limited by the amount of methanol that can diffuse from the

anode to the cathode through the membrane. By measuring the diffusion limited current and using Equation A-2 the rate of the methanol diffusion can be calculated.

$$Methanol\ consumption\ rate\ \left(\frac{mol\ CH_3OH}{s}\right) = \frac{load\ on\ the\ system\ (A)}{Faraday\ constant\ (s.\frac{A}{mol\ \bar{e}})} \times \frac{1}{6}\frac{mol\ CH_3OH}{mol\ \bar{e}} \quad \text{(A-2)}$$

The result of this experiment is shown in Figure A-2. Note that as it was expected, the diffusion limited current, in other words, methanol cross over, is directly related to the stack temperature and the solution concentration in the anode side.

The calculated methanol diffusion coefficient at a stack temperature of 50 ^{o}C is 5.649×10^{-10} (m^2/s) which is the average of the values is shown in Table A-1 In diffusion coefficient calculations, it was assumed that the methanol concentration at the ADL/ACL interface (Figure A-3) was equal to the bulk concentration and the methanol concentration at the membrane/CCL is equal to zero. So, the thickness in Table A-1 is the combined thickness of the membrane and the anode catalyst layer and the calculated diffusion coefficient is the combine diffusion coefficient for the membrane and the anode catalyst layer.

Theoretical Air Flow in the Cathode Channels

The limited oxygen flow to the cathode channels during the air-break is mainly consumed either for the cathode reaction (creating current), or in the crossover methanol combustion reaction. By knowing the diffusion coefficient of methanol through the membrane and also the available data for the current density during the air-break for a range of solution concentration, the required amount of the oxygen flow into the cathode channels during the break can be calculated. Figure A-4 shows the calculated

required oxygen flow through the cathode channels during the air-break for the stack operating temperature of 50^{o}C and 0.4 V/cell during the air-break. In Figure A-4, the red curve represents the required oxygen for the crossover methanol oxidation reaction. Clearly, as the solution concentration increases, a larger portion of the total required oxygen flow (the green curve) is consumed for the crossover methanol oxidation reaction. Also, the blue curve represents the required oxygen flow rate for the cathode reaction (oxygen reduction reaction) and it was calculated using the measured current density value for various solution concentrations and Equation A-2.

Measuring the Oxygen Flow Rate in the Cathode Channels

In order to measure the oxygen flow rate through the cathode channels during the air-breaks, a simple experiment was conducted. The cathode channels were initially purged with nitrogen, which causes the voltage to drop to a value around 50-100 mV/cell. Adding air flow to the nitrogen stream (Figure A-5) would increase the cathode potential therefore the stack voltage. However, if the stack voltage is set to constant value such as 0.4 V/cell (same as the conditions during the air-break), adding more air flow to the nitrogen stream initially brings up the voltage to 0.4 V/cell. Once the stack voltage raised to 0.4V/cell, adding more air flow to the nitrogen stream would generate more current. For any particular solution concentration, the air was gradually added to the nitrogen stream until the measured current density value for that particular solution concentration (Figure 4-9) was observed.

Figure A-6 shows the measured values for the oxygen flow rate through the cathode channels during the air-break period in comparison with the theoretical calculated values. The measured value curve has the same trend with the theoretical values, which proves the concept in terms of the effect of the methanol crossover on

current density during the air-break. However, the measured values are about 50% larger than the calculated values. This is attributed the fact that the theoretical values were calculated at the CCL/BL interface (Figure A-3) and the real values were measured in the cathode channels (right hand side of the barrier layer in Figure A-3). The barrier layer is basically a carbon paper layer (GDL) coated with several layers of Teflon-based coating and is impermeable to liquid water. Utilizing the barrier layer is a strategy to help the water management by keeping a portion of the water generated in the cathode reaction within the MEA and pushing it back to the anode through the membrane. Water management in DMFC's is not the topic of this work; however it is important to mention that the barrier layer is a clever strategy to help the water management, but on the other hand it reduces the oxygen accessibility to cathode catalyst layer. This clearly explains the reason why the measured values are higher than the theoretical calculated values.

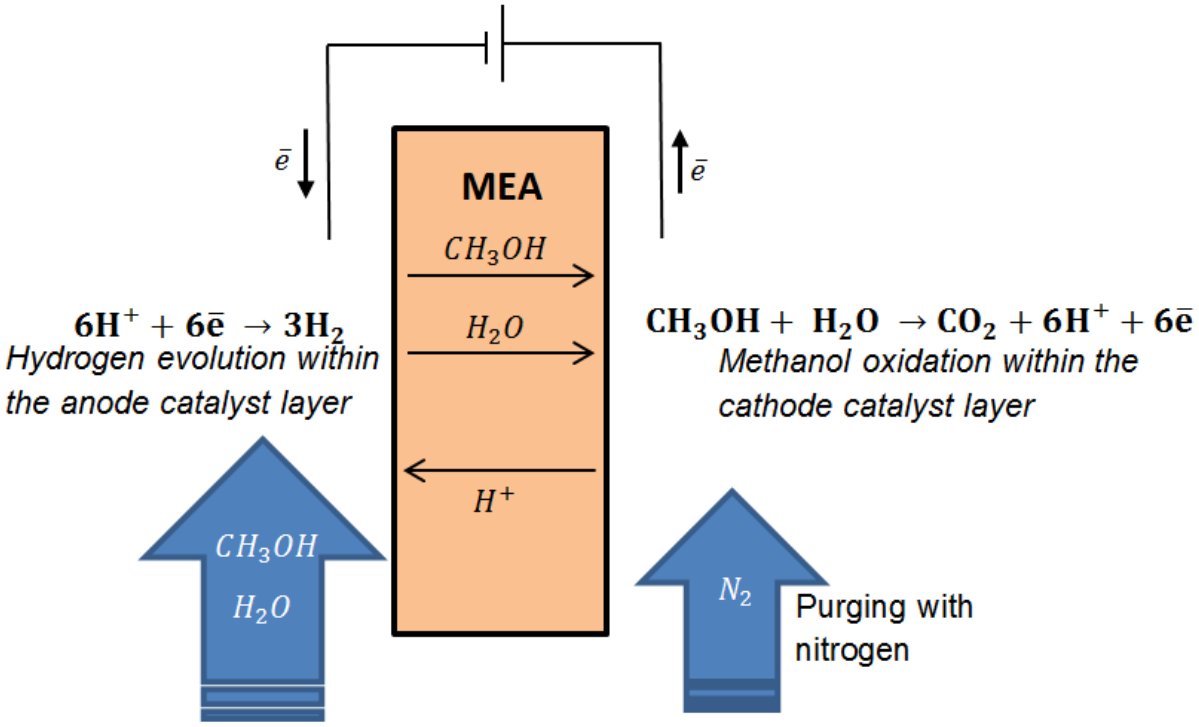

Figure A-1. Diffusion limited methanol oxidation current experiment.

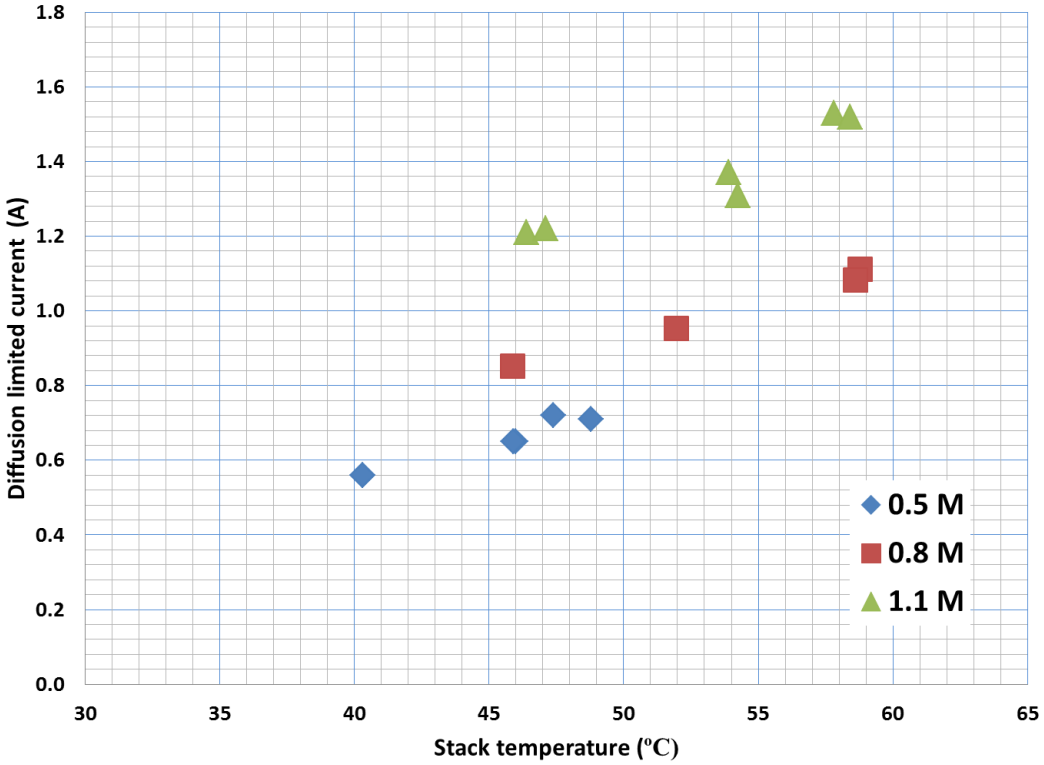

Figure A-2. Diffusion limited oxidation current at various anode solution concentrations and stack temperatures.

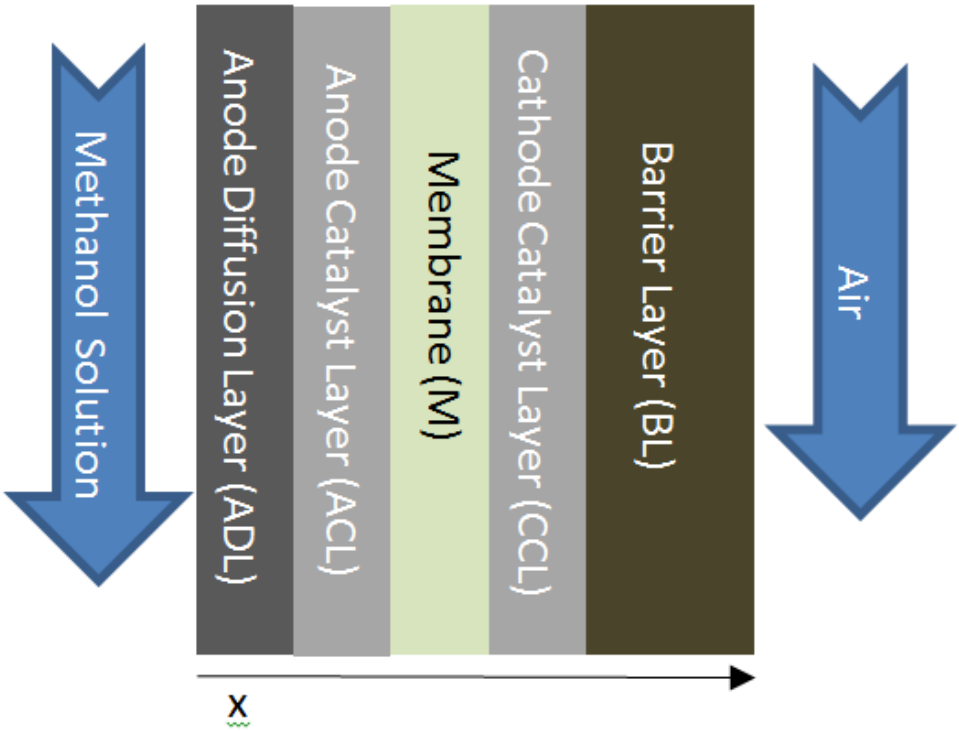

Figure A-3. The structure of MEA.

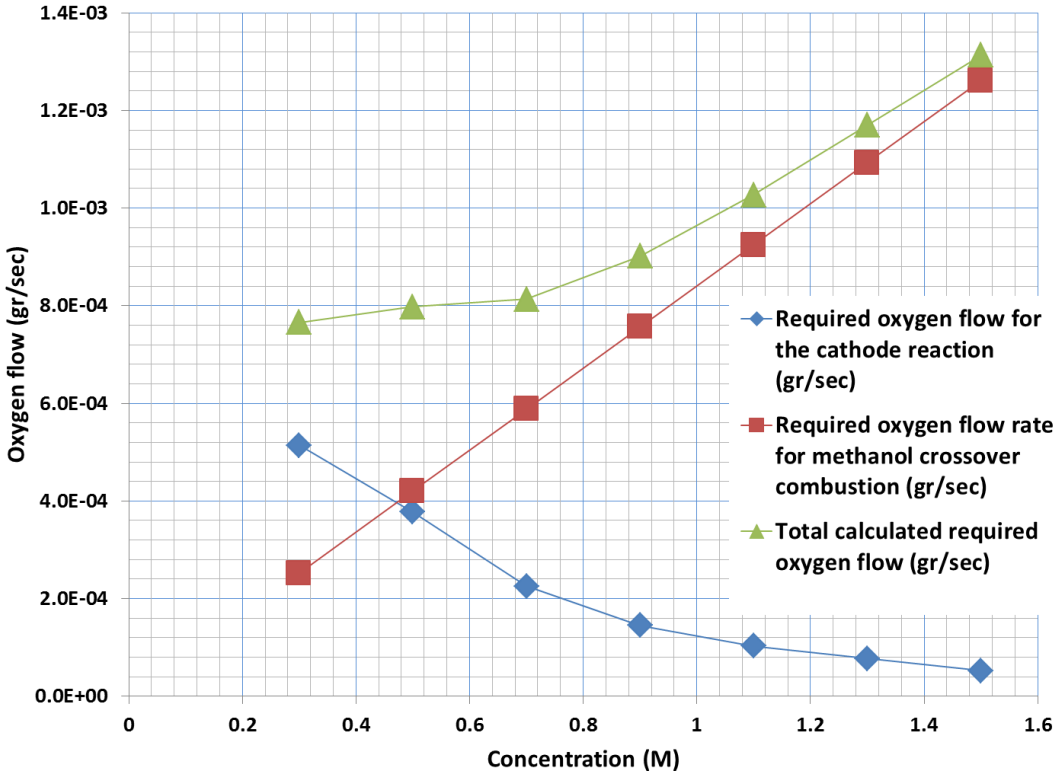

Figure A-4. Calculated required oxygen flow rate in the cathode channels during the air-break periods as a function solution concentration at 50°C and 0.4 V rest.

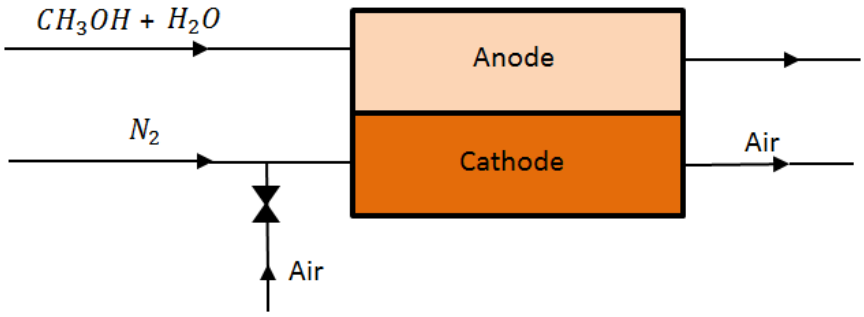

Figure A-5. Test set-up for measuring the air flow in the cathode channels during the air-break.

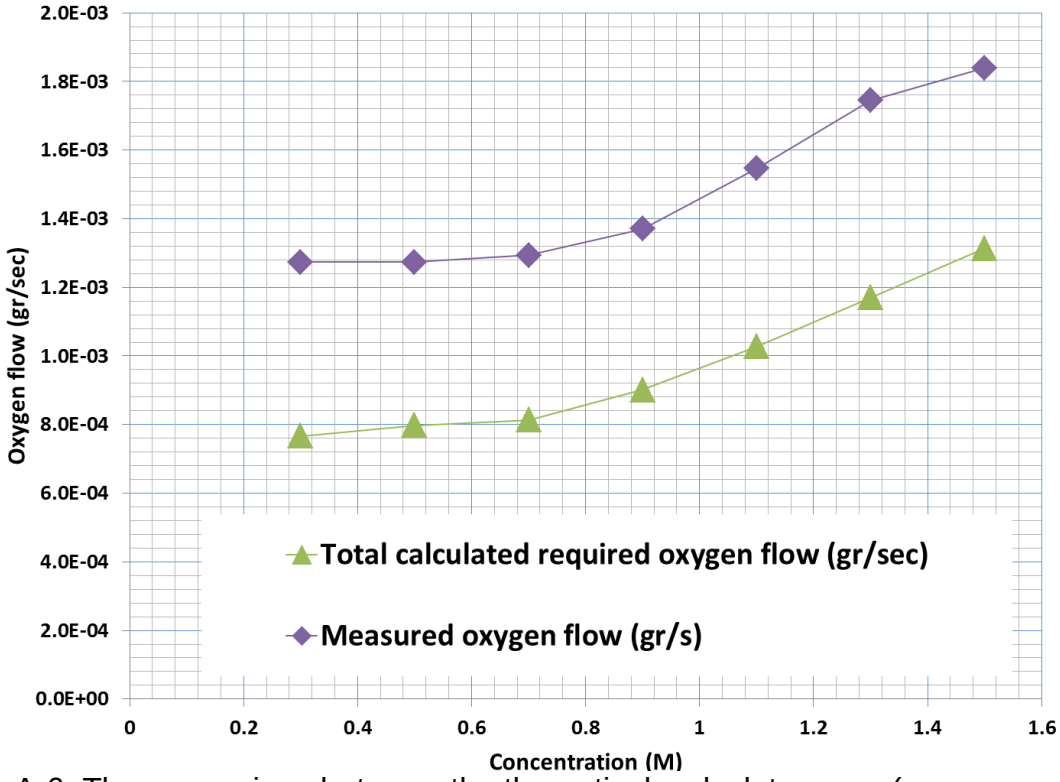

Figure A-6. The comparison between the theoretical calculate curve (green curve) and the measured values (blue curve) of the oxygen flow in the cathode channels during the air-break, at 50°C, and 0.4V rest.

Table A-1. Calculated methanol diffusion coefficient at 50 °C.

Solution concentration (M)	Diffusion limited current (A)	Methanol crossover flux (mol/m².s)	Thickness (m)	Diffusion coefficient (m²/s)
0.5	7.40E-01	8.25E-04	4.00E-05	6.60E-11
0.8	9.24E-01	1.03E-03	4.00E-05	5.15E-11
1.1	1.28E+00	1.43E-03	4.00E-05	5.20E-11

APPENDIX B
STATISTICAL ANALYSIS

Table B-1. Statistical analysis of the data shown in Figure 4-8.

Solution concentration (M)	Calculation based on	Probability that a sample falls in [m-σ, m+σ]	Probability that a sample falls in [m-2σ,m+2σ]	Probability that a sample falls in [m-3σ, m+3σ]
0.3	15th second	65.31%	97.96%	100.00%
	30th second	77.55%	100.00%	100.00%
	45th second	67.35%	100.00%	100.00%
0.5	15th second	71.43%	97.96%	100.00%
	30th second	79.59%	97.96%	100.00%
	45th second	85.71%	100.00%	100.00%
0.7	15th second	67.35%	100.00%	100.00%
	30th second	73.47%	100.00%	100.00%
	45th second	83.67%	100.00%	100.00%
0.9	15th second	71.43%	93.88%	100.00%
	30th second	73.47%	97.96%	100.00%
	45th second	59.18%	97.96%	100.00%
1.1	15th second	67.35%	95.92%	97.96%
	30th second	63.27%	97.96%	100.00%
	45th second	69.39%	97.96%	100.00%
1.3	15th second	69.39%	97.96%	100.00%
	30th second	63.27%	97.96%	100.00%
	45th second	59.18%	95.92%	100.00%
1.5	15th second	75.51%	97.96%	100.00%
	30th second	75.51%	93.88%	100.00%
	45th second	69.39%	97.96%	100.00%

LIST OF REFERENCES

[1] R. Rashidi, I. Dincer, G.F. Naterer, P. Berg, J.Power Sources, 187 (2009) 509-516.

[2] I. Horuz, J. Fletcher, C. C. Kuo, S. Credle, W. Lear (2008), pp. AIAA–2008–5667.

[3] R. O'Hayre, S. Cha, W. Colella, F. Prinz, Introduction, Fuel Cell Fundementals, 2nd ed., Wiley, 2009, pp. 3-25.

[4] J. Larminie, A. Dicks, Operational Fuel Cell Voltages, Fuel Cell Systems Explained, 2nd ed., Wiley, 2003, pp. 45-66.

[5] S.K. Kamarudin, F. Achmad, W.R.W. Daud, Int J Hydrogen Energy, 34 (2009) 6902-6916

[6] J. Chang, Y. Kuan, S. Lee, S. Lee, J.Power Sources, 184 (2008) 180-190

[7] L. Hansan, Z. Jiujun, Electrocatalysis of direct methanol fuel cells, Wiley, 2009, pp. 25.

[8] L. Maldonado, J. Perrin, J. Dillet, O. Lottin, J.Membr.Sci., 389 (2012) 43-56.

[9] V. Neburchilov, J. Martin, H. Wang, J. Zhang, J.Power Sources, 169 (2007) 221-238.

[10] P. Ferrin, A.U. Nilekar, J. Greeley, M. Mavrikakis, J. Rossmeisl, Surf.Sci., 602 (2008) 3424-3431.

[11] M. Hogarth, T. Ralph, In Johnson Mattey Technology Center, Reading, (2002) 146-164.

[12]Fletcher J. Advanced direct methanol fuel cell for mobile computing. 2012; Available at: http://www.hydrogen.energy.gov/pdfs/review12/h2ra004_fletcher_2012_p.pdf.

[13] H. Zhao, J. Shen, J. Zhang, H. Wang, D.P. Wilkinson, C.E. Gu, J.Power Sources, 159 (2006) 626-636

[14] T. Schultz, S. Zhou, K. Sundmacher, Chem.Eng.Technol., 24 (2001) 1223-1233.

[15] L. Hansan, Z. Jiujun, Electrocatalysis of direct methanol fuel cells, Wiley, 2009, pp. 503.

[16] C. Eickes, P. Piela, J. Davey, P. Zelenay, J. Electrochem. Soc., 153 (2006) A171-A178.

[17] J. Prabhuram, T.S. Zhao, H. Yang, J Electroanal Chem, 578 (2005) 105-112

[18] S.R. Narayanan, T.I. Valdez, W. Chun, Electrochem. Solid-State Lett., 3, issue 3 (2000) 117-120.

[19] S.R. Narayanan, W. Chun, T.I. Valdez, US Patent 6306285, (2001).

[20] J. Geng, X. Li, G. Sun, B. Yi, Sensors Actuators B: Chem., 147 (2010) 612-617.

[21] M.S. Lee, J. Sohn, J. Shim, W.M. Lee, Sensors Actuators B: Chem., 124 (2007) 323-328.

[22] K. Jeng, W. Huang, C. Chien, N. Hsu, Sensors Actuators B: Chem., 125 (2007) 278-283.

[23] T. Kumagai, T. Horiba, T. Kamo, S. Takeuchi, K. Iwamoto, K. Kitami, K. Tamura, US Patent 4810597, (1989).

[24] G. Luft, G. Starbeck, US patent 5,624,538, (1997).

[25] J. Zhang, K.M. Colbow, D.P. Wilkinson, J. Mller, US patent 6527943, (2003).

[26] Z. Guo, A. Faghri, Appl.Therm.Eng., 28 (2008) 1605-1613.

[27] K. Lee, J. Lee, S. Kim, B. Ju, Carbon, 49 (2011) 787-792.

[28] P. Enoksson, G. Stemme, E. Stemme, Sensors and Actuators A: Physical, 47 (1995) 327-331.

[29] D. Sparks, K. Kawaguchi, M. Yasuda, D. Riley, V. Cruz, N. Tran, A. Chimbayo, N. Najafi, Sensors and Actuators A: Physical, 145–146 (2008) 9-13.

[30] T. Sato, A. Chiba, R. Nozaki, Journal of Molecular Liquids, 101 (2002) 99-111.

[31] S. Doerner, T. Schultz, T. Schneider, K. Sundmacher, P. Hauptmann, Proceedings of the IEEE Sensors 2004. Vienna, Austria, vol. 2, pp. 639–641.

[32] M. Baldauf, W. Preidel, US Patent 6536262, (2003).

[33] R. Jiang, D. Chu, J. Electrochem. Soc. 151 (2004) A69–A76.

[34] A. Ozawa, A. Minamisawa, Jpn. J. Appl. Phys, 37 (1998) 2799.

[35] A. Rabinovich, D. Tulimieri, US Patent 6748793, (2004).

[36] C.C. Sung, Y.L. Tseng, Y.F. Chiang, C.Y. Chen, Sensors and Actuators A: Physical, 161 (2010) 101-107.

[37] A. Rabinovich, E. Diatzikis, J. Mullen, D. Tulimieri, US Patent 6815682, (2004).

[38] J.P. Longtin, C.H. Fan, Microscale Thermophys. Eng. 2 (1998) 261–272.

[39] H. Kodama, S. Kitajima, T. Suga, Japanese patent JP3251745, (1991).

[40] Baldauf, US Patent 20020148284, (2002).

[41] J. Kondoh, S. Tabushi, Y. Matsui, S. Shiokawa, Sensors Actuators B: Chem., 129 (2008) 575-580.

[42] Q. Mao, U. Krewer, Electrochim.Acta, 68 (2012) 60-68.

[43] Y. Chiu, H. Lien, J.Power Sources, 159 (2006) 1162-1168.

[44] K. Shen, C. Wan, Y. Wang, T.L. Yu, Y. Chiu, J.Power Sources, 195 (2010) 4785-4795.

[45] T.J. Ha, J. Kim, H. Joh, S. Kim, G. Moon, T. Lim, C. Han, H.Y. Ha, Int J Hydrogen Energy, 33 (2008) 7163-7171.

[46] S. Arisetty, C.A. Jacob, A.K. Prasad, S.G. Advani, J.Power Sources, 187 (2009) 415-421.

[47] C.Y. Chen, D.H. Liu, C.L. Huang, C.L. Chang, J.Power Sources, 167 (2007) 442-449.

[48] C.L. Chang, C.Y. Chen, C.C. Sung, D.H. Liou, J.Power Sources, 164 (2007) 606-613.

[49] C.L. Chang, C.Y. Chen, C.C. Sung, D.H. Liou, J.Power Sources, 182 (2008) 133-140.

[50] C.L. Chang, C.Y. Chen, C.C. Sung, D.H. Liou, C.Y. Chang, H.C. Cha, J.Power Sources, 195 (2010) 1427-1434.

[51] W. Harrington, Investigation of direct methanol fuel cell voltage response for methanol concentration sensing, 2012, University of Florida.

[52] C.O. Bennet, J.E. Myers, Molecular diffusion and diffusivity, Momentum, heat, and mass transfer, 2nd ed., McGraw-Hill, 1974, pp. 481-491.

[53] S.C. Thomas, X. Ren, S. Gottesfeld 2, P. Zelenay, Electrochim.Acta, 47 (2002) 3741-3748.

BIOGRAPHICAL SKETCH

Amir Reza Shoraka was born in Tehran, Iran in 1983. In 2009, he graduated with a bachelor degree in mechanical engineering from the University of North Florida. His interest in thermal sciences and renewable energy led him to start graduate school with focus on thermal sciences and working as a graduate research assistant under guidance of Dr. James Fletcher for a direct methanol fuel cell project at the University of North Florida. Amir graduated with a master degree in mechanical engineering from the University of Florida in summer of 2012.